

**Response to the Reviewer #1 comments for the manuscript “Erythematul ultraviolet irradiation trends in the Iberian Peninsula from 1950 to 2011” By R. Román et al. in ACPD**

First, we are really grateful for the effort of Reviewer #1 and her/his review in detail. Reviewer comments are in black font (RC), and author comments (AC) in red font.

Author’s answer to Reviewer

RC: 1. The present paper presents a reconstruction of erythematul ultraviolet radiation for the Iberian peninsula for the period 1950 to 2011. The authors mention in the introduction that in previous investigations UV ER irradiation was only reconstructed at Valladolid since 1991 and at two other sites for a time period starting in 1950 but only for the summer months. The present reconstruction was performed for 9 spanish locations and showed an increase of 6.5% between 1950 and 2011. The UVER irradiation over the open human body was also calculated by multiplying daily UVER irradiation by the daily open body fraction which is a function of air temperature and wind. An increase of 12.5% between 1950 and 2011 was obtained. Considering the fact that already existing reconstructions from literature performed for the Iberian peninsula for the period from 1950 to now were only performed for the summer months, the present paper could contain some new innovative results. The authors should however stress more on the new findings of the present work as compared to the papers by Bilbao et al. (2011) and Anton et al. (2011).

AC: We are agreed with the reviewer, the present paper could contain some new innovative results because the previous analyses were not done from 1950 at annual, winter, spring and autumn. A comparison with the results of Bilbao et al. (2011) and Antón et al. (2011) was carried out at Section 4.1.4 (UVER trends: Other periods) in the previous version. The new findings are also mentioned in the text (especially Section 4.1.4); in fact reviewer summarized some of them, hence, in order to stress more on the new findings, we include in the introduction (in the objectives paragraph) the next sentence:

*“The annual and seasonal (not only summer) UVER trends at the Iberian Peninsula from 1950 are a novel issue of this paper, since these trends were not yet calculated in previous studies.”*

RC: 2. The present study is one of the few studies, that I know, that include the open body fraction in the trend analysis. It is for me however still questionable how to interpret the open body erythemal UV values: the relevance of this quantity mainly pertains to the vitamin D production of the body and not to other uv related risks, since as soon as one part of the body is not covered by clothes it is at risk. It does not matter how much of the body is not protected in this case.

AC: We would like point out that the reviewer comment evidences the novelty of the paper, since this paper is the first using the open body fraction with erythemal UV radiation. Reviewer is right, as soon as one part of the body is not covered by clothes it is at risk, but on the other hand, if all body is covered (open body fraction equal to 0), the risk is null even for extreme high UV-Index.

WHO (2002) indicated that the risk of adverse health effects from UV radiation exposure is cumulative, hence we don't try to quantify the risk to produce sunburn (like UV-Index) but we want to quantify the UVER dose received by human skin. The portion of damaged skin will be higher when the open body fraction will be higher. As an example, we know the case of a 69-year-old man presented with a 25-year history of gradual, asymptomatic thickening and wrinkling of the skin on the left side of his face (Gordon and Brieva, 2012); his left side was exposed to UV radiation causing skin damage due to the cumulative UV effect, but if a more portion of his skin was also exposed to the same radiation, then more skin will be damaged.  $UVER_{ob}$  evidences in a certain way how much portion of the skin is damaged.

We also assume that the size of sunburn is important; for example, two persons in a beach, one with a t-shirt but the other without t-shirt; both irresponsibly decided take a nap leaving their backs exposed to the same UV radiation; after the nap both had sunburn but the redness skin of the person with t-shirt was the arms while the person without t-shirt had redness skin in the arms and his full back. We considered that the damage of UV radiation over the person without t-shirt (more redness area) was higher, and it happened because the  $UVER_{ob}$  received by the person without t-shirt was also higher.

In order to clarify this issue, we have changed some sentences of Section 4.2.2:

*“UVER irradiation quantifies the toxicity of solar radiation over human skin. However, if the human body is totally covered by clothes or anything else, the skin will not be affected by sun exposure even for high UVER irradiation values. Therefore, in order to find a new variable which quantifies the UVER dose received by human skin, the UVER*

*over open body ( $UVER_{ob}$ ) is defined as the UVER radiation multiplied by the open body fraction.  $UVER_{ob}$  irradiation, measured in  $Jm^{-2}$  per open body unit, physically means the daily UVER irradiation received over the naked skin of a human who is exposed to sun the whole day. The open body fraction is usually multiplied by the UV radiation weighted by the vitamin D synthesis action spectrum (e.g., Chubarova and Zhdanova, 2013), but not by UVER radiation. The damage of UV over human skin is cumulative (WHO, 2002), and  $UVER_{ob}$  can be used to evidences how much portion of skin is damaged or how much bigger is the redness skin after an overexposure to sun.”*

We still think that the UVER over open body is an interesting, novel and relevant magnitude, but it can be controversial. Anyway, we would like remark that if the reviewers still think that  $UVER_{ob}$  is not useful or necessary in this paper, we can remove this part (Section 4.2) in a second review process.

*WHO (World Health Organization): Global Solar UV Index: A Practical Guide, 28 pp., ISBN 92-4-159007-6, Geneva, Switzerland, 2002.*

*Gordon, J. R. S. and Brieva, J. C.: Unilateral Dermatoheliosis, N. Engl. J. Med., 366:e25, doi:10.1056/NEJMicm1104059, 2012.*

RC: 3. P.11: You should clearly mention what could be the result of a homogeneity test e.g. to find instrumentation/measurement problems, or is it only to find some trends such as the global dimming? When looking at fig. 2: at the station of A Coruna the end of 70ths and beginning of 80ths look very strange. The same remark applies to the peak in Madrid in the 70ths.

AC: The main purpose of the homogeneity tests is to obtain a statistical reference about the quality of the series. These tests give information about changes in instrumentation or any problem; we mainly look for this information in order to know if the series are useful or we need apply any correction. But we are lucky because these tests also give information about break points and changes in trends, and we use this information too. Therefore we use the tests mainly to study the quality of the series but also to detect changes in trends, like the reviewer mentioned. In order to clarify this, we added the next sentence in the new manuscript:

*“The homogeneity tests are mainly applied in order to know whether the series are valid for trend studies or, on the contrary, they are not valid due to instrumentation/measurement problems; additionally, the homogeneity tests can provide information about break points in some climatic trends.”*

Regarding the peaks of A Coruña and Madrid, they can look strange, but the homogeneity tests indicate that the annual UVER series from 1950-2011 at Madrid is inhomogeneity-free; for A Coruña just one month shows inhomogeneity in the 1950-1984 period (none for 1985-2011). In fact, the inhomogeneity detected at A Coruña could be related to the lack of data from the beginning of 70s to mid 70s. Therefore, these results point out that UVER series have the enough homogeneity to be considered as quality series (independently of their strange shape).

Other minor comments

RC: P.2, line 28: “Changes in aerosols led to alterations in the presence and microphysical properties of clouds: : :..”???

AC: This sentence has been replaced by:

*“Changes in aerosols can modify the microphysical properties of clouds”*

RC: P.4 line 3: “A further aim is to propose and study a new variable to quantify the UVER dose that reaches the naked human body exposed to sun” I would suggest to change “the naked human body exposed to sun” with “ the body parts exposed to the sun (not covered by clothes)”

AC: The sentence has been replaced as reviewer suggests.

RC: P5 line 10: up the present => up to the present

AC: Done.

RC: P.6 line 4 and 6: Chuvaroba => Chubarova

AC: Done.

RC: P.6 line 25: Roman(2014) which one of the Roman(2014) publications?

AC: It has been corrected. The reference of Román (2014) is a PhD thesis which is not any Román et al. (2014a, b, c, or d) previously cited.

RC: P.8, line 17: bins => intervals

AC: Done.

RC: P.13 line 29: please say in one sentence in what consists the methodology of Walker (2010).

AC: It has been explained adding the next sentence:

*“...the methodology used by Walker (2010), who plotted the trends as points which type depends on the trend significance and he also added the 95% confidence intervals as error bars.”*

RC: I do not think that you need to show figure 4. There is no difference between the trend of these three quantities because mean wind speed has probably not changed very much during this period. It would be enough to mention this in one sentence

AC: We are agreed with reviewer, hence we removed the effective temperature, and the open body fraction panels of the new paper, but we still think that the plot with mean temperature can be interesting. Mean temperature evolution is useful to understand the variation in the UVER irradiation over open body. How there is no difference between the trend of these three quantities, we show just one: mean temperature, and the remaining are mentioned in the text:

*“The behaviour of  $t_{eff}$ , and  $S$  (not shown) is similar since  $S$  is directly connected with  $t_{eff}$ , and  $t_{eff}$  with  $T_m$  (Sect. 2).”*

**Response to the Reviewer #2 comments for the manuscript “Erythemal ultraviolet irradiation trends in the Iberian Peninsula from 1950 to 2011” By R. Román et al. in ACPD**

We acknowledge Reviewer #2 for her/his review in detail (of this manuscript and the other mentioned in the review). Reviewer comments are in black font (RC), and author comments (AC) in red font.

Author’s answer to Reviewer

RC: 1. To begin with, I want to acknowledge the editor and the authors that I am currently also reviewing another manuscript by the same authors submitted to Atmospheric Research (title: “Comparison of nine different models to reconstruct erythemal ultraviolet radiation”).

These two manuscripts are connected in the following way: the manuscript submitted to Atmospheric Research (denoted #1) presents and compares models for reconstructing UV radiation, while the present manuscript (denoted #2) presents an analysis of the resulting UV time series, calculated using two UV reconstruction methods included in #1, over the Iberian peninsula since 1950.

My main concern, which I already mention in my initial quick review, is that there may be overlap between these papers by the same authors. In principle, it could be possible to keep these two manuscripts apart and publish them as separate papers. However, if they are to be published separately, the authors need to make it perfectly clear what has been done in each paper and how the papers connect to each other, why each of the paper is needed and what their respective scientific contribution is.

Manuscript #2 (this review) is still not clearly explaining the differences and connections to manuscript #1. Sections 2 and 3 include lengthy passages which are more or less the same in both manuscripts. This is not acceptable.

AC: Our initial intention was develop a paper (manuscript #1) focused on the reconstruction model development and a depth comparison of reconstructed series with quality measurements. This was motivated by the intention to publish a second paper (manuscript #2, this one) exclusively focused on the analysis of the reconstructed series (trends, influence of uncertainty, etc.). We thought that it could avoid the need of a really extensive paper. However, it had some problems as reviewer said. Some parts of

the papers were similar even repeated, and the connection between them was not enough clear.

As a solution we decided remove the manuscript #1 (Atmospheric Research; title: “Comparison of nine different models to reconstruct erythemal ultraviolet radiation”), and we include the model development and a quick comparison with measurements in the new manuscript at Section 3.2. It avoids the problems about overlap between both papers and the not clear connection between them.

However, rejecting the first paper about reconstruction models, the depth analysis about models vs. measurements has been strongly reduced (the paper will be too much extensive). Anyway, the mentioned problems have been solved by this way.

RC: 2. Another important concern with this manuscript (#2) is the use of the open body fraction. I agree with the other reviewer that it is not clear how to interpret the open body erythemal UV series. If the open body UV is to be included in the study, it would require much more motivation, background, and discussion on why it is a useful quantity, for example, for epidemiological studies.

AC: We are agreed with both reviewers, this variable  $UVER_{ob}$ , should be more explained and discussed. In this sense, the paragraph has been changed by:

*“UVER irradiation quantifies the toxicity of solar radiation over human skin. However, if the human body is totally covered by clothes or anything else, the skin will not be affected by sun exposure even for high UVER irradiation values. Therefore, in order to find a new variable which quantifies the UVER dose received by human skin, the UVER over open body ( $UVER_{ob}$ ) is defined as the UVER radiation multiplied by the open body fraction.  $UVER_{ob}$  irradiation, measured in  $Jm^{-2}$  per open body unit, physically means the daily UVER irradiation received over the naked skin of a human who is exposed to sun the whole day. The open body fraction is usually multiplied by the UV radiation weighted by the vitamin D synthesis action spectrum (e.g., Chubarova and Zhdanova, 2013), but not by UVER radiation. The damage of UV over human skin is cumulative (WHO, 2002), and  $UVER_{ob}$  can be used to evidences how much portion of skin is damaged or how much bigger is the redness skin after an overexposure to sun.”*

The changes and motivations are included in the response to the reviewer #1, but we included the same text for the reviewer #2 convenience.

WHO (2002) indicated that the risk of adverse health effects from UV radiation exposure is cumulative, hence we don't try to quantify the risk to produce sunburn (like UV-Index) but we want to quantify the UVER dose received by human skin. The portion of damaged skin will be higher when the open body fraction will be higher. As an example, we know the case of a 69-year-old man presented with a 25-year history of gradual, asymptomatic thickening and wrinkling of the skin on the left side of his face (Gordon and Brieva, 2012); his left side was exposed to UV radiation causing skin damage due to the cumulative UV effect, but if a more portion of his skin was also exposed to the same radiation, then more skin will be damaged.  $UVER_{ob}$  evidences in a certain way how much portion of the skin is damaged.

We also assume that the size of sunburn is important; for example, two persons in a beach, one with a t-shirt but the other without t-shirt; both irresponsibly decided take a nap leaving their backs exposed to the same UV radiation; after the nap both had sunburn but the redness skin of the person with t-shirt was the arms while the person without t-shirt had redness skin in the arms and his full back. We considered that the damage of UV radiation over the person without t-shirt (more redness area) was higher, and it happened because the  $UVER_{ob}$  received by the person without t-shirt was also higher.

We still think that the UVER over open body is an interesting, novel and relevant magnitude, but it can be controversial. Anyway, we would like remark that if the reviewers still think that  $UVER_{ob}$  is not useful or necessary in this paper, we can remove this part (Section 4.2) in a second review process.

*WHO (World Health Organization): Global Solar UV Index: A Practical Guide, 28 pp., ISBN 92-4-159007-6, Geneva, Switzerland, 2002.*

*Gordon, J. R. S. and Brieva, J. C.: Unilateral Dermatoheliosis, N. Engl. J. Med., 366:e25, doi:10.1056/NEJMicm1104059, 2012.*

RC: 3. As mentioned in my previous review, there is also a need to consider more carefully what really can be concluded based on the work presented. Example: how much can be concluded about the role of aerosols and clouds from the reconstructed UV series which is based on climatological aerosols as input?



AC: We try to consider more carefully the conclusions of the paper. In fact there is a section named “Factors not taken into account” which evidences the considered approximations and how they could influence on the obtained results.

Regarding the use of a climatological aerosol, there is a sentence in the manuscript which tries to justify it:

*“The lack of AOD data earlier 2000 led to use a climatological table which does not contain the aerosol changes in the 1950-2011 period. However the aerosol effect is included the SW and F measurements (like clouds) and, as a first approximation, the reconstruction models transfer this effect to the UVER radiation.”*

First, the UV series are based on climatological aerosols, because, as expected, there are not measurements of aerosols from 1950. Hence we need use this approximation. But the UV series are also based on SW (or F) measurements, which are affected by aerosols and clouds. The effect of aerosol and clouds into the SW and F measurements is transferred to the reconstructed UVER series. Therefore we suppose that reconstructed UVER series include the aerosol effect.

In addition, the uncertainty in the cloudless simulations (given by aerosol uncertainty and monthly variability) is taken into account, and this uncertainty is around 50% (Román et al., 2014c) for every month, which is probably higher than the changes in AOD along the last 6 decades. This uncertainty is included in the reconstructed UVER series, and section 4.1.5 (Effect of UVER uncertainty on trends) gives the trends which are significant even taking into account the uncertainty. It means that the aerosol variability has not been considered directly in the cloudless simulations but this variability is taken into account through uncertainty and SW and F measurements.

About the role of aerosol and clouds, we assume that UVER changes are mainly caused by TOC, aerosol, and clouds. We have TOC data from 1950, then we can quantify the ozone effect; but we have not data for clouds and aerosols before 2000, then we cannot discern between the role of aerosols and clouds, but we can assume that the role of clouds and aerosols together is the role of all components minus the role of ozone. Therefore we talk about the clouds and aerosol effect together, but we don't discern between aerosols and clouds.

*Román, R., Bilbao, J., and de Miguel, A.: Uncertainty and variability in satellite-based water vapor column, aerosol optical depth and Angström Exponent, and its effect on radiative transfer simulations in the Iberian Peninsula, Atmos. Environ., 89, 556-569, 2014c.*

RC: 4. Finally, I find that some parts of the manuscript are difficult to read and would therefore benefit from language checking and additional checks on the preciseness and logic of the expression (one example: section 2.2 introduces the data used, but it is often not clear whether the values have been used to create a monthly climatology or as a more realistically varying time series).

AC: We take this comment into account and we have tried to improve the new version for an easy reading with better preciseness and logic. Regards the language, the first version was revised in detail by a professional and native speaker (we can provide the invoice if it will be necessary). Regarding the example of the reviewer, we would like point out that section 2.2 only introduces the data used, but this section is not for the explanation about how they are used. In fact, Section 3.1 indicates how the data are used for the simulations:

*“These vertical profiles were rescaled with monthly climatological tables of water vapour, AOD at 443 nm, Angström Exponent, and SSA (at 354 nm for UVER simulations and at 500 nm for SW ones). These climatology tables (one per location and variable) comprised 12 monthly averaged (using all available data) values for each variable, said climatological tables being available in Román et al. (2014c). The daily TOC at each location was included in the inputs, changing the value for each location on each day. Finally, the spectral surface albedo values were also monthly averaged, these monthly values being linearly interpolated to obtain surface albedo at each wavelength to be then used as input in the radiative transfer code”*

The ozone is used as daily input and the remaining as monthly climatology tables; but the climatology tables are calculated using the data mentioned in Section 2.2.

RC: 5. Because of the overlap between #1 and #2 it is difficult to give a standard recommendation on the scale minor / major revisions / rejection. In any case, the manuscript(s) require more work before publication.

AC: This problem has been solved removing the paper #1 as we indicate in the first point of this review.

1 **Changes noted in the new version of the manuscript**  
2 **“Erythemal ultraviolet irradiation trends in the Iberian**  
3 **Peninsula from 1950 to 2011”**

4 This document includes the new version of the manuscript titled “Erythemal ultraviolet  
5 irradiation trends in the Iberian Peninsula from 1950 to 2011” submitted to ACP journal. The  
6 changes regards the previous version in ACPD are marked in red font. The major change has  
7 been the next:

8 Section 3.2 has been completely changed. In this new version Section 3.2 includes two new  
9 Figures and one Table (Figures 2 and 3, and Table 2). This information has been added in the  
10 Section 3.2 because the reference to an “under review” paper of the same authors has been  
11 deleted (in fact this “under review” paper was removed in order to avoid overlapping).

12  
13  
14  
15  
16  
17  
18  
19  
20  
21  
22  
23

# Erythematul ultraviolet irradiation trends in the Iberian Peninsula from 1950 to 2011

R. Román<sup>1</sup>, J. Bilbao<sup>1</sup>, and A. de Miguel<sup>1</sup>

[1]{University of Valladolid, Laboratorio de Atmósfera y Energía, Department of Applied Physics, Valladolid, Spain.}

Correspondence to: R. Román (robertor@fa1.uva.es)

## Abstract

Erythematul ultraviolet (UVER) irradiation was reconstructed at nine Spanish locations, with series starting around 1950 in at least five places. Each series was checked by applying homogeneity tests in order to discard non-homogeneous series. Available series were used to create an averaged Iberian Peninsula UVER series. Results indicate that annual UVER irradiation in the Iberian Peninsula increased by  $155 \text{ Jm}^{-2}$  (6.5%) between 1950 and 2011 due to a decrease observed in atmospheric ozone rather than changes in aerosol and clouds. Annual UVER irradiation increased by  $135 \text{ Jm}^{-2}$  (5.6%) between 1985 and 2011, mainly due to changes in aerosol and clouds. UVER irradiation over the open human body ( $\text{UVER}_{\text{ob}}$ ) was calculated by multiplying daily UVER irradiation by the daily open body fraction, a function of air temperature. Annual  $\text{UVER}_{\text{ob}}$  increased by 12.5% between 1950 and 2011 in the Iberian Peninsula, half of the increase being caused by temperature changes, and the other half by ozone changes. Annual  $\text{UVER}_{\text{ob}}$  in the Iberian Peninsula increased by a total of 10.1% between 1985 and 2011, with 20.7%, 35.1% and 44.2% of this increase being caused by changes in ozone, aerosol and clouds, and temperature, respectively.

## 1 1 Introduction

2 Among other effects, ultraviolet (UV) radiation, which is a part of total solar shortwave (SW)  
3 radiation, produces harmful effects on human skin, such as erythema (sunburn) induction  
4 (UNEP, 2003). On the other hand, UV radiation exposure can be positive, for example by  
5 contributing towards human Vitamin D synthesis (Webb, 2006). The effectiveness of UV  
6 radiation in producing erythema on human skin is usually quantified by the erythemal action  
7 spectrum (McKinlay and Diffey, 1987), and the UV radiation weighted by this spectrum is  
8 erythemal ultraviolet (UVER) radiation.

9 The damage caused to human skin by UVER radiation is cumulative and is proportional to  
10 exposure time (WHO, 1995). It is therefore important to know both present-day as well as  
11 past UVER radiation levels in order to estimate future epidemiological data related to diseases  
12 caused by sun exposure. However, it was not until the 1980s that the first UVER  
13 measurement databases appeared, to be followed by more in the 1990s (den Outer et al.,  
14 2010). In fact, the first UVER records in Spain commenced in late 1995, and were taken in  
15 Madrid by the Spanish Meteorological Agency (AEMet). In order to obtain longer and older  
16 UVER data, several authors have reconstructed UVER data in the past using other available  
17 records (Lindfors et al., 2003, 2007; den Outer et al., 2005, 2010; Rieder et al., 2008; Walker,  
18 2010; Antón et al., 2011a; Bilbao et al., 2011 among others).

19 UVER radiation is sensitive to factors such as ozone, clouds, and aerosol particles in the  
20 atmosphere. Over the last few decades, the presence of these factors in the atmosphere has  
21 changed, and might have affected past UVER levels.

22 SW radiation decreased between 1950 and the mid 1980s in the Northern Hemisphere, a  
23 phenomenon known as "global dimming" (Stanhill and Cohen, 2001). SW radiation began to  
24 increase in the mid 1980s in the Northern Hemisphere, a phenomenon known as "global  
25 brightening" (Wild et al., 2005). Dimming and brightening were caused because aerosol loads  
26 increased in the Northern Hemisphere between 1950 and the mid 1980s absorbing and  
27 scattering (aerosol direct effect) more radiation, although after the mid-1980s the aerosol load  
28 started to decrease (Wild, 2009, 2012). **Changes in aerosols can modify the microphysical  
29 properties of clouds** (aerosol indirect effect), since aerosols act as condensation nuclei, which  
30 contributes to enhance the dimming and brightening phenomena. The mentioned aerosol and  
31 cloud changes might cause variations in the amount of UVER radiation reaching Earth.

1 Dimming and brightening phenomena were observed in the Iberian Peninsula by Sánchez-  
2 Lorenzo et al. (2007, 2013a, b).

3 The atmospheric total ozone column (TOC) evidenced major depletion after the late 1970s up  
4 to the mid 1990s due to strong atmospheric emission of halogen gases between the 1960s and  
5 1980s (WMO, 2011). TOC evolution in the Iberian Peninsula was studied in depth by Román  
6 et al. (2014d) in the dimming and brightening periods, with usually negative but not  
7 significant trends being reported in both periods, and a statistically significant trend of -  
8  $0.73\%dc^{-1}$  in the annual TOC between 1950 and 2011. These TOC changes have no  
9 significant influence on SW radiation, although they might prove extremely relevant for  
10 UVER evolution over the last few decades, marking the difference between the SW and  
11 UVER trends in the past.

12 Another atmospheric variable to undergo changes in recent decades is air temperature, which  
13 rose after the 1970s due to the increase in the anthropogenic greenhouse gas emissions  
14 warming the Earth by the greenhouse effect, giving rise to “global warming” (IPCC, 2007).  
15 Vicente-Serrano et al. (2013) studied the daily mean temperature in the Iberian Peninsula, and  
16 reported non-significant and negative trends in the dimming period, and significant and  
17 positive trends in the brightening period. Changes in air temperature have no direct influence  
18 on UVER radiation, although they can affect people’s sun exposure habits.

19 Many authors have found statistically significant positive trends over the last decades for  
20 UVER radiation at different places in the following European countries: Austria, Czech  
21 Republic, Finland, Greece, Germany, the Netherlands, Norway, Sweden, and Switzerland  
22 (Lindfors et al., 2003; 2007; Rieder et al., 2008; Walker, 2010; den Outer et al., 2010;  
23 Krzyscin et al., 2011). They often attribute increased UVER radiation to ozone depletion  
24 since the late 1970s and to the reduction in the amount of aerosols in the atmosphere during  
25 the brightening period.

26 UVER radiation presents high levels in the Iberian Peninsula due to the great height the sun  
27 reaches, making it an interesting area to study the evolution of UVER radiation. However, in  
28 the Iberian Peninsula, UVER radiation has only been reconstructed at Valladolid, since 1991  
29 (Bilbao et al., 2011), and at Badajoz and Cáceres (only in the summer months) since 1950  
30 (Antón et al., 2011a), a significant rise in UVER radiation levels having been reported at the  
31 three sites.

1 Recently the same authors obtained from 1950 to 2011, at the Iberian Peninsula, the TOC  
2 trends in Román et al. (2014d); and the SW and temperature trends in Román et al. (2014a),  
3 but not the UVER trends due to the lack of UVER data. As a first step, the same authors  
4 (Román et al. 2014b) simulated the UVER irradiance under cloudless conditions at the Iberian  
5 Peninsula with a radiative transfer model, using as inputs monthly climatological tables of  
6 aerosols, water vapour, etc. (which were obtained in Román et al., 2014c); they also  
7 characterized the uncertainty of these simulations caused by the monthly variability and  
8 uncertainty of the inputs. These cloudless simulations are useful to reconstruct UVER  
9 radiation under all conditions (e.g., Lindfors et al., 2003, 2007; den Outer et al., 2005;  
10 Walker, 2010; Bilbao et al., 2011).

11 Therefore, in this framework, the main objectives of the present paper are: to reconstruct  
12 UVER irradiation series since 1950 using new and optimised reconstruction models (based on  
13 cloudless UVER simulations) and data at certain Spanish locations over the Iberian Peninsula;  
14 and to analyse their evolution and trends. The annual and seasonal (not only summer) UVER  
15 trends at the Iberian Peninsula from 1950 are a novel issue of this paper, since these trends  
16 were not yet calculated in previous studies. A further aim is to propose and study a new  
17 variable to quantify the UVER dose that reaches the body parts exposed to the sun (not  
18 covered by clothes). Another goal is to quantify the role of the changes in aerosols and clouds  
19 (both together), ozone, and temperature in the changes of UVER on an exposed body.

20 The paper is structured as follows: Sect. 2 shows the relevant information concerning the  
21 locations, the instrumentation, and the explanation of all the data used. The methods used to  
22 obtain the reconstructed UVER series are developed and explained in detail in Sect. 3. Sect. 4  
23 presents the main results for the evolution and trends of UVER and UVER on an exposed  
24 body in recent decades. The factors not taken into account in the work are mentioned in Sect.  
25 5. Finally, Sect. 6 summarises the main results and conclusions.

26

## 27 **2 Place, instrumentation, and data**

### 28 **2.1 Places and instrumentation**

29 All data used in this paper were taken at nine Spanish radiometric stations located in the  
30 Iberian Peninsula. These locations are marked in Fig. 1 and their coordinates are also shown  
31 in Table 1. The Iberian Peninsula is well covered by these locations. One of these stations is



1 controlled by the University of Valladolid and is located in the village of “Villalba de los  
 2 Alcores” (de Miguel et al. 2012). The rest are controlled by the Spanish Meteorological  
 3 Agency (Moreta et al., 2013). Hourly UVER and SW irradiance were measured at all these  
 4 stations, although sunshine duration and temperature were not measured at the Villalba  
 5 station. Therefore, the sunshine duration and meteorological variables, as with temperature,  
 6 measured at the Valladolid Airport AEMet station were thus considered the same as at the  
 7 Villalba station, since the two stations are located just a few kilometres away from each other.  
 8 Hourly UVER irradiance was recorded at the nine locations using UVB-1 pyranometers  
 9 (Yankee Environmental Systems Inc.). These pyranometers were periodically calibrated by a  
 10 two-step method (Vilaplana et al., 2009), which provides a combined uncertainty (68%  
 11 confidence) of between 5.4% and 8.0% for the measured hourly UVER data (Hülsen and  
 12 Gröbner, 2007). This uncertainty was considered the maximum (8.0%) in this work. The  
 13 oldest UVER data recorded in Spain date from 1<sup>st</sup> November 1995 and continue **up to the**  
 14 **present** day at the Madrid station.

15 Hourly SW irradiance was initially measured at each location using a CM6B pyranometer  
 16 (Kipp & Zonen), whose spectral response ranges from 305 nm to 2,800 nm. The expanded  
 17 uncertainty (95% confidence) of the hourly SW recorded by this pyranometer is 8%, and was  
 18 the expanded uncertainty assumed by all available hourly SW measurements even when more  
 19 recent records were taken using improved pyranometers (displaying less uncertainty). The  
 20 oldest SW data in Spain date from 11<sup>th</sup> July 1973 and continue up to the present day at the  
 21 Madrid station.

22 In general, it was not possible to obtain information on the instruments used for sunshine  
 23 duration records at the various stations, although most were probably Campbell-Stokes  
 24 heliographs (Sánchez-Lorenzo et al., 2007). This heliograph comprises a spherical lens which  
 25 concentrates direct radiation from the sun onto a dark paper card, which is burned when direct  
 26 radiation exceeds a certain threshold. The combined uncertainty of the sunshine duration  
 27 records was assumed to be 15 minutes (0.25 h). The daily sunshine fraction (F) is the ratio of  
 28 the measured sunshine duration to the same sunshine duration under cloudless conditions  
 29 ( $SunDu_{cl}$ ). This variable was calculated by the following equation (Iqbal, 1983):

$$30 \quad SunDu_{cl} = \frac{24}{\pi} \arccos\left(\frac{\cos(\theta_s) - \sin(\delta)\sin(\phi)}{\cos(\delta)\cos(\phi)}\right) \quad (1)$$

1 where  $\text{SunDu}_{\text{cl}}$  is in hours,  $\delta$  is the solar declination,  $\Phi$  is the location latitude, and  $\theta_S$  is the  
2 solar zenith angle (SZA) at sunset and sunrise (equal to  $87^\circ$  in this case).  $\text{SunDu}_{\text{cl}}$  was  
3 calculated between the solar zenith angle of  $87^\circ$  near sunrise and the SZA equal to  $87^\circ$  near  
4 sunset, since direct solar radiation might not be enough to burn the dark paper card even  
5 under cloud free conditions for a SZA below  $87^\circ$ . The oldest available F data in Spain date  
6 from 1<sup>st</sup> January 1920 and continue up to the present day at the Madrid station. F data have  
7 been available at certain locations (A Coruña, Madrid, San Sebastián, Tortosa, and Villalba)  
8 since the 1950s.

9 Daily mean temperature ( $T_m$ ), daily mean wind speed ( $V_m$ ), and relative humidity (RH) at  
10 7:00, 13:00, and 18:00 (GMT) were also recorded at the AEMet stations. The daily effective  
11 temperature ( $t_{\text{eff}}$ ), which is mainly a function of air temperature with a correction on wind  
12 velocity for negative temperatures, was calculated with the mentioned variables (Chubarova  
13 and Zhdanova, 2013). The  $t_{\text{eff}}$  can be parameterized by the following equation for the daily  
14 mean temperatures below  $0^\circ\text{C}$  (Chubarova and Zhdanova, 2013):

$$15 \quad t_{\text{eff}} = T_m + (4.27V_m^{-0.229} - 10) \quad (2)$$

16 where  $T_m$  is the daily mean air temperature in degrees Celsius at 2 m, and  $V_m$  is the wind  
17 velocity in  $\text{ms}^{-1}$  at 10 m. The daily effective temperature for  $T_m$  values above  $20^\circ\text{C}$  was  
18 assumed equal to the heat index (Steadman, 1979). The Heat index is an index that combines  
19 air temperature and relative humidity in an attempt to determine the human-perceived  
20 equivalent temperature, and it was calculated by an interpolation with the  $T_m$  and the averaged  
21 value of the three daily HR measurements (at 07:00, 13:00, and 18:00). The daily effective  
22 temperature was assumed to be equal to  $T_m$  for  $0^\circ\text{C} < T_m < 20^\circ\text{C}$ , and when HR or  $V_m$   
23 measurements were not available. Chubarova and Zhdanova (2013) assumed that the open  
24 body fraction (S), which can be interpreted as the fraction of human body not covered by  
25 clothes, directly depends on the effective temperature:

$$26 \quad S = 0.141 \exp(0.041 t_{\text{eff}}) \quad (3)$$

27 The daily open body fraction was calculated for each day at each location taking into account  
28 the daily effective temperature calculated with the measured AEMet data.

29 The instruments used to take all the mentioned measurements were well calibrated on a  
30 regular basis, following World Meteorological Organization (WMO) recommendations  
31 (Webb et al., 2006; WMO, 2008) for instrument maintenance, and involved: bubble levelling

1 of the instruments, cleaning domes, monitoring and replacing desiccant, etc. Quality control  
2 of UVER, SW, and F data was applied to all available data in order to reject spurious and  
3 outlier data. Daily UVER and SW irradiation data were obtained integrating the hourly values  
4 each day.

## 5 **2.2 Other data**

6 Other atmospheric data were also obtained and downloaded in order to calculate UVER and  
7 SW irradiance under cloudless conditions in Sect. 3.1. Some of these data are described in this  
8 section. Daily aerosol optical depth (AOD) at 433 nm and 670 nm (“MISR-Terra Prod.ver.31:  
9 MIL3DAE.004” product) from the MISR instrument (Multi-angle Imaging  
10 SpectroRadiometer) were obtained at each location from 2000 to 2012. The Angström  
11 Exponent was directly calculated using both AOD values. The daily water vapour column (w)  
12 (“MODIS-Terra Ver. 5.1: MOD08\_D3.051” product) from MODIS (MODerate resolution  
13 Imaging Spectroradiometer) was also obtained at each location between 2000 and 2012. AOD  
14 and water vapour column data were downloaded from the GIOVANNI application (GES-  
15 DISC Interactive Online Visualization ANd aNalysis Infrastructure;  
16 <http://disc.sci.gsfc.nasa.gov/giovanni>) as an averaged 0.2°x0.2° square centred at each location  
17 (Acker and Leptoukh, 2007). The aerosol single scattering albedos (SSA) at 354 nm and 500  
18 nm retrieved from the OMI (Ozone Monitoring Instrument) instrument between 2004 and  
19 2011 were also obtained for all locations as overpass files available at AVDC (Aura  
20 Validation Data Center). These data are the same as those used by Román et al. (2014c), who  
21 calculated the uncertainty of some of these products in the Iberian Peninsula. The combined  
22 uncertainty of AOD at 433 nm and 670 nm is 0.074 and 0.054, respectively. The combined  
23 uncertainty of the Angström Exponent is below 0.5 when AOD at 433 nm is above 0.25,  
24 except for high Angström Exponent values. The combined uncertainty of the water vapour  
25 column is between 0.38 cm (w=0.5 cm) and 0.52 cm (w=3 cm).

26 A daily total ozone column series for 1950 to 2011 was available for each location. These  
27 series comprised different databases: ground-based ozone; ozone retrieved from TOMS (Total  
28 Ozone Mapping Spectrometer) instrument on board Nimbus-7, Meteor-3, and Earth-probe  
29 satellites; TOC from OMI; retrieved TOC from GOME (Global Ozone Monitoring  
30 Experiment) and GOME-2 instruments on board ERS-2 and MetOp-A satellites; and  
31 reconstructed ozone data from the COST-726 project (Krzyscin, 2008; [www.cost726.org](http://www.cost726.org)).  
32 The construction of these TOC series was explained by Román et al. (2014d) who, by means

1 of an intercomparison with ground measurements, calculated that the combined uncertainty of  
2 the daily TOC values of these series was around 10.5 DU.

3 Surface albedo data between 2000 and 2011 were obtained each eight days at seven  
4 wavelength ranges (459-479 nm, 545-565 nm, 620-670 nm, 841-876 nm, 1230-1250 nm,  
5 1628-1652 nm, and 2105-2155 nm) from the MCD43A3 product of MODIS instruments  
6 (Schaaf et al., 2002). In addition, daily surface albedo at 360 nm between 1957 and 2002 was  
7 obtained from the COST-726 project database as an interpolation at each location of the  
8 available data grid (Schwander et al., 1999; Tanskanen, 2004). More information concerning  
9 the albedo and ozone data used in this work is available in Román et al. (2014d).

10

### 11 **3 Reconstructed UVER series**

#### 12 **3.1 Simulations under cloudless conditions**

13 Global, diffuse and direct horizontal UVER and SW irradiance were simulated under  
14 cloudless conditions using a radiative transfer model (UVSPEC/libRadtran) from 1950 to  
15 2011 each hour for all locations shown in Fig. 1. UVSPEC is the main tool of the libRadtran  
16 (version 1.7 in this work) software package developed by Mayer and Kylling (2005). For  
17 UVER simulations, irradiance was calculated each 1 nm from 280 nm to 400 nm under cloud-  
18 free conditions using the “cdisor” solver with six streams (Buras et al., 2011) and the  
19 “SUSIM SL2” extraterrestrial spectrum (Van Hoosier et al., 1988), these obtained values then  
20 being weighted with the erythemal action spectrum. For SW simulations, the model was run  
21 under cloudless conditions using the “twostr” solver (Kylling et al., 1995), the extraterrestrial  
22 spectrum from Kurucz (1992), and the pseudo-spectral k-distribution “SBDART” from  
23 Ricchiazzi et al. (1998). Irradiance was calculated from 305 nm to 800 nm in 2 nm **intervals**,  
24 from 800 nm to 1,600 nm in 5 nm **intervals**, and from 1,600 to 2,800 nm in 10 nm **intervals**,  
25 these spectral values then being spectrally integrated to obtain SW irradiance. An hourly  
26 (UVER or SW) irradiance value was simulated at a fixed SZA given by the averaged cosine  
27 of the SZA over the hour.

28 The UVSPEC model was run using standard vertical profiles. A mid-latitude summer  
29 atmosphere with spring-summer aerosol profiles was used as input for the months from May  
30 to October, with a mid-latitude winter atmosphere with fall-winter aerosol profiles being  
31 selected for the other months (Anderson et al., 1987; Shettle, 1989). These vertical profiles

1 were rescaled with monthly climatological tables of water vapour, AOD at 443 nm, Angström  
2 Exponent, and SSA (at 354 nm for UVER simulations and at 500 nm for SW ones). These  
3 climatology tables (one per location and variable) comprised 12 monthly averaged (using all  
4 available data) values for each variable, said climatological tables being available in Román et  
5 al. (2014c). The daily TOC at each location was included in the inputs, changing the value for  
6 each location on each day. Finally, the spectral surface albedo values were also monthly  
7 averaged, these monthly values being linearly interpolated to obtain surface albedo at each  
8 wavelength to be then used as input in the radiative transfer code.

9 Both the combined and the expanded uncertainty of all simulations were calculated using the  
10 results obtained by Román et al. (2014b), who calculated the maximum variations in  
11 simulated UVER and SW irradiance caused by the uncertainty of the inputs. Simulated hourly  
12 SW and UVER values were also compared with global SW and UVER irradiance  
13 measurements under cloudless conditions by Román et al. (2014b). It was found there was  
14 better agreement for low SZA values, and that the differences between simulations and  
15 measurements were in agreement within the uncertainty. Daily UVER and SW irradiation  
16 were calculated for each day at each location by adding the simulated hourly UVER and SW  
17 values and multiplying the result by 3600 s (1 hour). The uncertainties of these daily values  
18 were also calculated. Román et al. (2014b) compared these simulations with measured  
19 irradiation under cloudless conditions, with better agreement being found for the spring and  
20 summer months. For all months and locations together, a mean bias error (MBE) of -0.1% and  
21 a root mean square error (RMSE) of 3.6% for the SW case, and an MBE of 2.9% and an  
22 RMSE of 7.7% for the UVER case, were also reported.

## 23 **3.2 Reconstruction models**

### 24 **3.2.1 Cloud Modification Factor**

25 The cloud modification factor (CMF) is defined as the ratio between measured radiation and  
26 simulated radiation under cloudless conditions:

$$27 \quad CMF_R = \frac{R_{me}}{R_{cl}} \quad (4)$$

28 where R can be SW or UVER, the “me” index indicating the measured R value, and the “cl”  
29 index being for simulated R radiation under cloudless conditions. CMF can be calculated for

1 hourly irradiance or daily irradiation values. CMF is a useful variable to quantify cloudiness,  
2 CMF near 1 indicating cloudless conditions, CMF close to 0 being for high overcast  
3 cloudiness, and CMF above 1 indicating enhancement effects (Sabburg and Parisi, 2006;  
4 Sabburg and Calbó, 2009; Piedehierro et al., 2014). CMF for SW ( $CMF_{SW}$ ) is usually  
5 different for UVER ( $CMF_{UVER}$ ). The relationships between  $CMF_{UVER}$  and other variables, like  
6  $CMF_{SW}$ , are an important research topic since they prove useful for reconstructing UVER  
7 data. If a relationship between  $CMF_{UVER}$  and  $CMF_{SW}$  is given by a function  $f$ :

$$8 \quad CMF_{UVER} = f(CMF_{SW}) \quad (5)$$

9 then UVER radiation can be obtained when the measured SW radiation, UVER and SW  
10 simulations under cloudless conditions, and the  $f$  function are known:

$$11 \quad UVER = f(CMF_{SW}) UVER_{cl} \quad (6)$$

12 where UVER is the calculated UVER radiation, and  $UVER_{cl}$  is the simulated UVER under  
13 cloudless conditions. The main goal of this section is to obtain relationships such as the one  
14 given by Eq. (5) in order to reconstruct UVER data as a function of other variables as in Eq.  
15 (6).

### 16 **3.2.2 Model based on hourly SW irradiance measurements**

17 Some UVER reconstruction models are based on different measured variables (Calbó et al.,  
18 2005), with several UVER reconstruction models being based on SW radiation  
19 measurements, which were normally measured before UVER (Bodeker and McKenzie, 1996;  
20 Kaurola et al., 2000; Matthijsen et al., 2000; den Outer et al., 2000, 2005; Lindfors et al.,  
21 2007; Walker, 2010; Antón et al., 2011b; Bilbao et al., 2011). The data used to obtain a model  
22 based on SW were the measured values when both SW and UVER irradiance measurements  
23 were available. A total of 294,047 pairs of data (SW and UVER) were available for SZA  
24 below  $85^\circ$  taking all locations into account. Hourly CMF was calculated for hourly SW and  
25 UVER irradiance with the mentioned available data. The reconstruction model proposed in  
26 this paper was based on the model developed by Bilbao et al. (2011), which suggests the next  
27 relationship:

$$28 \quad CMF_{UVER} = CMF_{SW}^{c+d \cos(SZA)} \quad (7)$$

29 where  $c$  and  $d$  are two parameters which can be calculated by a least square fit. Bilbao et al.  
30 (2011) calculated  $c$  and  $d$  using all data measured at one location and did not take uncertainty

1 into account in the variables of Eq. (7). The method to calculate c and d can be improved  
2 considering a similar number of data for different cloudiness and SZA conditions, and taking  
3 into account the uncertainty in these data. To this end, a dataset of  $CMF_{UVER}$ - $CMF_{SW}$  pairs of  
4 data was selected in this paper.

5 All available data pairs of  $CMF_{UVER}$ - $CMF_{SW}$  from all locations were divided into data groups  
6 taking into account the cosine of SZA. Eighty-seven data groups were obtained separated by  
7 intervals of the cosine of SZA, from 0.095 to 0.965 in 0.01 steps. Each data group was  
8 divided into a further 15 subgroups considering the  $CMF_{SW}$  value in the intervals from 0 to  
9 1.5 in 0.1 bins. A total of 1305 subgroups were available. Fifty pairs of  $CMF_{UVER}$ - $CMF_{SW}$   
10 data were chosen randomly for each subgroup. Some groups with high  $CMF_{SW}$  values had  
11 fewer than 50 data. Finally, 49,777 data pairs were randomly selected. This method of  
12 choosing data ensures that the number of data selected is similar and is representative for any  
13 cloudiness and SZA condition.

14 The combined uncertainty of each selected data was known; hence the c and d parameters of  
15 Eq. (7) were calculated by the weighted least square method using the 49,777 chosen data.  
16 The weight in the fit was the inverse of the square combined uncertainty. Uncertainty in SZA  
17 was considered null. The result of the fit gave a c value equal to 0.6106 with a combined  
18 uncertainty of 0.0014, and a d value equal to 0.358 with a combined uncertainty of 0.002.  
19 These calculated values are different to those obtained by Bilbao et al. (2011). Once the c and  
20 d values were calculated, the f function of Eq. (6) can be expressed as:

$$21 \quad f(CMF_{SW}) = (CMF_{SW})^{(0.6106 \pm 0.0014) + (0.358 \pm 0.002) \cos(SZA)} \quad (8)$$

22 UVER irradiance can be reconstructed using Eq. (8) in Eq. (6) taking into account cloudless  
23 simulations and measured SW irradiance. This model for reconstructing UVER irradiance  
24 was called “M-SW”.

### 25 **3.2.3 Model based on daily sunshine fraction measurements**

26 Another variable used to reconstruct UVER radiation is sunshine fraction (Lindfors et al.,  
27 2003), due to the availability of longer series than SW; it has the advantage to reconstruct  
28 older data. The sunshine fraction represents the fraction of day when sun was not blocked by  
29 clouds. Therefore, by way of an initial approach, daily direct (on horizontal) UVER  
30 irradiation ( $UVER^{dir}$ ) can be expressed as:



1  $UVER^{dir} = UVER_{cl}^{dir} F$  (9)

2 where  $UVER_{cl}^{dir}$  is the daily direct UVER irradiation simulated under cloudless conditions on  
3 horizontal surface. Assuming Eq. (9), daily global UVER irradiation can thus be expressed as  
4 the sum of the direct (on horizontal surface) and diffuse ( $UVER^{dif}$ ) components:

5  $UVER = UVER_{cl}^{dir} F + UVER^{dif}$  (10)

6 As a second approximation, daily diffuse UVER irradiation can be assumed as a function ( $g$ ),  
7 which depends on the daily diffuse UVER under cloudless conditions ( $UVER_{cl}^{dif}$ ) and on  $F$ :

8  $UVER^{dif} = g(UVER_{cl}^{dif}, F)$  (11)

9 Eq. (11) in Eq. (10) gives:

10  $UVER = UVER_{cl}^{dir} F + g(UVER_{cl}^{dif}, F)$  (12)

11 Global UVER irradiation can be obtained through  $F$  measurements and cloudless simulations  
12 using Eq. (12) once the  $g$  function is known. The  $g$  function can be calculated by  $F$  and UVER  
13 measurements:

14  $g = UVER - UVER_{cl}^{dir} F$  (13)

15 In order to calculate the  $g$  values a new dataset was chosen made up of daily UVER  
16 irradiation and  $F$  measurements. Days without SW, UVER or  $F$  measurements were discarded  
17 in the new dataset. Available data (all locations) were then divided by the season: winter  
18 (January, February, and December), spring (March, April, and May), summer (June, July, and  
19 August) and autumn (September, October, and November). 10% of the available data for each  
20 season were randomly selected and used to obtain the  $g$  function. Figure 2 shows the values  
21 of  $g$  calculated by Eq. (13) as a function of  $UVER_{cl}^{dif}$  for four  $F$  intervals. The  $g$  values  
22 increase linearly with cloudless diffuse UVER irradiation, showing a correlation coefficient  
23 ( $r$ ) above 0.87 for all  $F$  intervals. Moreover, the dependence of  $g$  on  $UVER_{cl}^{dif}$  varies with  $F$ ,  
24 and shows a higher slope when  $F$  increases. This result indicates that the  $g$  function could be  
25 expressed as:

26  $g = a(F) + b(F) \cdot UVER_{cl}^{dif}$  (14)

27 where  $a$  and  $b$  are two parameters which depend on  $F$ . Both the  $a$  and  $b$  parameters were  
28 calculated through a least square fit using the same data as in Fig. 2, but for the following  $F$



1 intervals:  $F=0$ ,  $0<F<0.2$ ,  $0.2\leq F<0.4$ ,  $0.4\leq F<0.6$ ,  $0.6\leq F<0.8$ ,  $0.8\leq F<1$ ,  $F\geq 1$ . The values  
2 obtained are shown in Fig. 3 (left and middle panels) with their combined uncertainty as a  
3 function of  $F$ . The  $b$  parameter increases with  $F$ , although the  $a$  parameter does not present a  
4 clear dependence on  $F$ , and is always near to zero. This result indicates that the  $a$  parameter  
5 can be assumed null, transforming Eq. (14) into:

$$6 \quad g = B(F) UVER_{cl}^{dif} \quad (15)$$

7 where  $B$  is a new parameter which also depends on  $F$ . The  $B$  parameter was calculated by a  
8 least square fit using the same data as in the  $a$  and  $b$  parameter calculations. Fig. 3 (right  
9 panel) shows the  $B$  values and their combined uncertainty. This parameter increases with  $F$ ,  
10 and is close to 1 when  $F$  tends to 1. Uncertainty is around 0.2 except for  $F$  equal to 1, when it  
11 strongly increases up to 0.55 (caused in part by the high uncertainty in  $UVER_{cl}^{dir}$ , which is not  
12 reduced multiplying by  $F$ ). The  $B$  value can be obtained by interpolating the values of Fig. 3  
13 for an  $F$  measurement. This interpolated value of  $B$  can be used to retrieve global UVER  
14 irradiation taking into account Eq. (15) in Eq. (12):

$$15 \quad UVER = UVER_{cl}^{dir} F + B(F) UVER_{cl}^{dif} \quad (16)$$

16 The method for retrieving global UVER irradiation finding a  $B$  value by an  $F$  measurement  
17 interpolation in Fig. 3 and using this  $B$  value with the measured  $F$  and cloudless simulations  
18 in Eq. (16) was called “M-F” in this paper.

### 19 **3.2.4 Models vs. measurements**

20 Hourly UVER irradiance was reconstructed with model M-SW using the available data which  
21 were not used to develop the model M-SW. Twenty-five UVER data (three days) were  
22 rejected applying a new quality control. A total of 220,105 pairs of measured ( $UVER_{me}$ ) and  
23 reconstructed ( $UVER_{mo}$ ) UVER irradiance data were available for each model considering  
24  $SZA<80^\circ$ . These data pairs were used to quantify the agreement between UVER reconstructed  
25 by model and measured UVER irradiance. The combined and expanded uncertainty of all  
26 reconstructed values were calculated deriving the equations of the model and taking into  
27 account the uncertainty in the used measurements and cloudless simulations. Table 2 shows  
28 the MBE and the RMSE obtained in the comparison between the reconstructed and measured  
29 hourly UVER values. The model M-SW slightly overestimates the measurements showing a  
30 MBE of 1.6% ( $0.7 \text{ mWm}^{-2}$ ); the RMSE was 15.8% ( $6.2 \text{ mWm}^{-2}$ ). A depth analysis (not

1 shown) indicated that model M-SW fit better within the measurements for  $SZA < 55^\circ$   
2 (RMSE < 10%); the MBE is close to 0% for  $SZA < 75^\circ$ ; the best RMSE and MBE values  
3 appears for  $CMF_{SW}$  values between 0.2 and 1.1.

4 In order to quantify the agreement between the models and the daily UVER measurements, all  
5 data not used to develop models M-F (90% of data per season) were selected. The  
6 reconstructed UVER irradiance these days was integrated to obtain the reconstructed daily  
7 UVER irradiation by model M-SW. Daily irradiance was also reconstructed by model M-F.  
8 The available number of pairs of data for reconstructed and measured daily UVER irradiation  
9 was 21,349 as can be seen in Table 2. Table 2 also shows that model M-SW fit better (with a  
10 RMSE of 8.4%) within measurements than model M-F (RMSE higher than 20%); moreover,  
11 model M-F overestimates the daily measurements showing a MBE of 5.1%. RMSE and MBE  
12 were also calculated for different F intervals (not shown) and model M-SW presents RMSE  
13 values lower than 10% and MBE closest to 0% for all F intervals; model M-F show a good  
14 agreement with measurements for F higher than 0.5 but RMSE and MBE increases when F  
15 decreases.

16 All available data (used and not used to develop models) were used to obtain daily UVER  
17 irradiation, and these values were monthly averaged (at least 25 days per month) for each  
18 location and year. The same monthly averages were reconstructed with the models. The MBE  
19 and RMSE obtained using the monthly averages of reconstructed and measured UVER  
20 irradiation are shown in Table 2. These values are similar for both models, being the MBE  
21 around 2% and RMSE around below 6.5%. The number of data for the models is different due  
22 to the lack of F data in some periods at Madrid in the 2000s decade. Monthly averages were  
23 used to obtain the annual averaged (always with all 12 months available) UVER irradiation  
24 value at each location. Annual reconstructed and measured data were compared also in Table  
25 2 showing the statistical estimators of the comparison. Both models present a good agreement  
26 with measurements being RMSE lower than 3% and MBE below 1% in absolute value. 95%  
27 of the reconstructed annual UVER data with model M-SW shows a difference below 5% with  
28 the measurements.

29 Finally, as an important result (not shown), the differences between measured and  
30 reconstructed values are in agreement within uncertainty for both models and for all temporal  
31 resolutions. Model M-F measurements are not the best for reconstructing daily UVER  
32 irradiation although it evidences great agreement with monthly and annual averaged

1 measurements. A depth comparison not shown in this paper about these models can be found  
2 in Román (2014).

### 3 **3.3 Final reconstructed series**

4 Hourly UVER irradiance was reconstructed at each location, when hourly SW records were  
5 available, using the method referred to as M-SW. Daily reconstructed UVER irradiation was  
6 obtained by integrating the hourly reconstructed values. Table 1 (M-SW column) shows the  
7 number of daily UVER irradiation data reconstructed by the model based on SW records.  
8 This number is around 10,000 (27 years) for A Coruña, Cáceres, and Murcia, and is over  
9 13,000 (36 years) for Madrid. Villalba shows the lowest number of reconstructed UVER data  
10 by this model due to the scant number of SW records at this location. When SW records were  
11 not available, UVER irradiation was reconstructed using the method M-F and based on F  
12 measurements. Table 1 (M-F column) shows the number of daily UVER irradiation data  
13 reconstructed by the model based on F records. This number varies with the location, and is  
14 higher for Villalba, San Sebastián, and Tortosa. The reconstructed daily UVER irradiation  
15 series were completed with daily measured UVER irradiation when SW and F records were  
16 not available. The number of measured data used to form the UVER series is shown in Table  
17 1 (Measured data column). This number of data is low compared to the other reconstructed  
18 data, is less than 20 at all locations, and is zero in Murcia and Villalba. Finally, a long-term  
19 daily UVER irradiation series was obtained at each location using models and measurements.  
20 The total number of data of these series and the year of the first UVER irradiation value are  
21 shown in Table 1. A Coruña, Madrid, San Sebastián, and Villalba show UVER series with  
22 more than 20,000 data, all commencing in the 1950s. The lowest number of daily UVER data  
23 is around 10,000 for Cáceres and Murcia, whose UVER series commenced in the mid 1980s.  
24 The combined uncertainty of all daily UVER irradiation values of the obtained series was also  
25 calculated taking into account the uncertainty in the cloudless simulations and measured  
26 values.

## 1 4 Results and discussion

### 2 4.1 UVER irradiation

#### 3 4.1.1 Anomalies and homogeneity

4 Monthly averages of daily UVER irradiation were calculated using the available reconstructed  
5 series taking into account at least 20 daily UVER data per month, year, and location. The  
6 monthly series obtained were deseasonalized calculating their monthly anomalies considering  
7 the reference period from 1985 to 2011. UVER anomaly (A) in month “m” and year “y” is  
8 thus calculated as:

$$9 \quad A_{m,y} = UVER_{m,y} - \frac{1}{N} \sum_{y'=1985}^{2011} UVER_{m,y'} \quad (17)$$

10 where N is the number of data used in the sum of Eq. (17). Monthly UVER irradiation  
11 anomalies were calculated for all months at all locations. The monthly anomalies of UVER  
12 irradiation at the nine locations were averaged, obtaining a new monthly series of anomalies  
13 representative of the Iberian Peninsula. This was then called the “Iberian Peninsula” series.  
14 Annual UVER anomalies were calculated averaging the monthly anomalies when at least six  
15 monthly data were available for each year. Seasonal anomalies were also calculated when at  
16 least two monthly data were available in winter (December, January, and February), spring  
17 (March, April, and May), summer (June, July, and August), and autumn (September, October,  
18 and November). Winter anomalies were calculated with the January and February anomalies  
19 for a specific year, together with the December anomaly of the previous year.

20 Homogeneity of all these averaged daily UVER irradiation anomaly series was tested in a  
21 similar way to the TOC and SW series analyzed by Román et al. (2014a, d). **The homogeneity  
22 tests are mainly applied in order to know whether the series are valid for trend studies or, on  
23 the contrary, they are not valid due to instrumentation/measurement problems; additionally,  
24 the homogeneity tests can provide information about break points in some climatic trends.** In  
25 this case, the null hypothesis assumes that a temporal series is homogenous, and this  
26 hypothesis was verified using the Standard Normal Homogeneity Test (SNHT), the Pettitt  
27 test, the Buishand test, and the Von Neumann ratio (Wijngaard et al., 2003). Hakuba et al.  
28 (2013) assumed that a temporal series is non-homogeneous when the null hypothesis is  
29 rejected with a confidence of 99% by at least three of the four mentioned tests. The four tests

1 were directly carried out on the annual UVER series. Eight (all except Madrid and Murcia) of  
2 the ten (nine locations plus the averaged Iberian Peninsula) annual series show non-  
3 homogeneity around the mid 1980s, which could be caused by a climate change in UVER  
4 from the dimming to brightening periods. Homogeneity analysis was thus performed for the  
5 same annual UVER series for the 1950-1984 and 1985-2011 periods. The first period  
6 evidences inhomogeneities in San Sebastián and A Coruña, and the second period is free of  
7 inhomogeneities. The same result was obtained by Román et al. (2014c) for the annual SW  
8 irradiation series.

9 The monthly series was also subjected to homogeneity analysis by applying the four tests to  
10 the synthetic reference series generated with UVER data from the other locations  
11 (Alexandersson and Moberg, 1997; Sánchez-Lorenzo et al., 2013c). No monthly UVER series  
12 shows inhomogeneities for the 1985-2011 period, and only one month shows inhomogeneity  
13 in Madrid and San Sebastián in the 1950-1984 period. These results thus indicate that all the  
14 UVER anomaly series can be considered homogeneous, or at least not inhomogeneous  
15 enough to change the UVER series values.

#### 16 **4.1.2 UVER temporal evolution**

17 Figure 4 shows the annual UVER daily irradiation anomaly series for the nine locations and  
18 the averaged Iberian Peninsula series. Anomalies are shown with their combined uncertainty.  
19 Figure 4 panels present a 21-year Gaussian low-pass filter to reduce noise in the evolution.  
20 Moreover, the linear trends calculated by the least square method are plotted for the 1950-  
21 2011, 1950-1984, and 1985-2011 periods. All annual UVER anomalies display an increase  
22 between 1950 and 2011, this increase also appearing from 1985 to 2011, except in A Coruña.  
23 However, in the 1950-1984 period, the annual UVER series which contains most data shows  
24 no increase. In fact, UVER irradiation shows a slight decrease in this period. San Sebastián is  
25 the location exhibiting the clearest change in UVER in the 1980s, which explains the break  
26 point detected in this location with the homogeneity tests. Román et al. (2014a) found that  
27 SW irradiation at the same locations decreased during the dimming period, and Román et al.  
28 (2014d) found that TOC decreased in the same period. These results indicate that UVER in  
29 the dimming period tended to decrease due to increased aerosol and clouds (as in SW  
30 irradiation) but that UVER tended to increase due to ozone depletion. The two effects offset  
31 one another, leading to little change in UVER irradiation over the dimming period.

1 An example of the compensatory effects between the impact of aerosol increase and ozone  
2 depletion can be seen after a major volcanic eruption during which vast amounts of gaseous  
3 compounds can be shot into the stratosphere. These are precursors for the atmospheric  
4 formation of sulphate aerosol particles which in turn provide surfaces for heterogeneous  
5 processes on polar stratospheric clouds in the lower stratosphere, enhancing ozone depletion  
6 (Peter, 1997; Solomon, 1999; Rieder et al., 2013). In sum, aerosol load increases and ozone  
7 decreases after a violent volcanic eruption. The volcanic eruptions at El Chichón (México)  
8 and Pinatubo (Philippines) in 1982 and 1991, respectively, are highlighted in Fig. 4. Román et  
9 al. (2014a) found that years after these eruptions, a reduction in SW irradiation due to the  
10 increase in sulphate aerosol particles is apparent. However, by contrast, UVER irradiation  
11 shows little increase in most of the panels in Fig. 4. The UVER increase is caused by the  
12 strong decrease in TOC after volcanic eruptions detected at these locations by Román et al.  
13 (2014d), which leads to an increase in UVER more than a UVER decrease caused by  
14 aerosols.

#### 15 **4.1.3 UVER trends: Dimming and brightening periods**

16 Figure 4 shows the annual UVER evolution and trends in qualitative but not quantitative  
17 terms. In order to quantify them, the temporal trends of the monthly, seasonal, and annual  
18 UVER anomaly series were assumed to be the trends obtained by the Theil-Sen (TS)  
19 estimator and its 95% confidence interval (95CI). The statistical significance of each  
20 calculated trend was evaluated by the non-parametric Mann-Kendall test, considering three  
21 types of trends: with a confidence of 99% ( $p < 0.01$ ), with a confidence of 95% but not 99%  
22 ( $p < 0.05$ ), or non-significant at least at 95% confidence ( $p \geq 0.05$ ). All these estimators were  
23 calculated following the methods of Gilbert (1987). If the Mann-Kendall test considered a  
24 trend as statistically significant with at least 95% confidence, this trend was then assumed to  
25 be just significant. A trend was only calculated when a series comprised more than 10 data.  
26  $TS_{o_3}$  is the TS trend calculated with the same UVER irradiation series but simulated under  
27 cloudless conditions. The  $TS_{o_3}$  value gives the UVER trend caused by changes in TOC  
28 because aerosol and clouds changes are not included in cloudless simulations.  $TS_{ac}$  is defined  
29 as TS minus  $TS_{o_3}$ , and represents the UVER trend brought about by changes in aerosol and  
30 clouds (both together).

31 The trends (and their significance and 95CI) of monthly, seasonal, and annual UVER  
32 irradiation series were calculated for all locations at three periods: 1950-1984 (considered as

1 the dimming period), 1985-2011 (considered as the brightening period), and 1950-2011. Fig.  
2 5 shows all these values following the methodology used by Walker (2010), who plotted the  
3 trends as points which type depends on the trend significance and he also added the 95%  
4 confidence intervals as error bars. The significant seasonal and annual trends are also shown  
5 in Table 3, which also shows  $TS_{O_3}$  and  $TS_{ac}$  trends. The most representative trends of the  
6 dimming period are those obtained for the San Sebastián, Madrid, Villalba, and Iberian  
7 Peninsula series, since they have fewer missing data. The mentioned series show no  
8 significant trends in the dimming period except San Sebastián, which evidences a significant  
9 trend of  $-211 \text{ Jm}^{-2}\text{dc}^{-1}$  ( $-7.7\%\text{dc}^{-1}$ ) in May, and an annual trend of  $-48 \text{ Jm}^{-2}\text{dc}^{-1}$  ( $-2.8\%\text{dc}^{-1}$ ).  
10 The negative annual trend found in San Sebastián is caused by changes in aerosol and clouds  
11 rather than ozone since  $TS_{ac}$  is much higher than  $TS_{O_3}$ . Román et al. (2014a) found many  
12 more significant trends in SW irradiation for the same locations during the dimming period,  
13 underpinning the key role played by ozone decrease in UVER trends during the dimming  
14 period.

15 The brightening period (1985-2011) has the advantage that all UVER series are complete.  
16 UVER trends are mainly significant in summer and in the annual series. All series, except for  
17 A Coruña and Madrid, present significant trends in summer, and are  $109 \text{ Jm}^{-2}\text{dc}^{-1}$  ( $2.5\%\text{dc}^{-1}$ )  
18 for the Iberian Peninsula series. The annual trend of the Iberian Peninsula series is  $50 \text{ Jm}^{-2}\text{dc}^{-1}$   
19 ( $2.1\%\text{dc}^{-1}$ ). The  $TS_{ac}$  and  $TS_{O_3}$  values in Table 3 reveal that UVER irradiation increased in the  
20 brightening period due to a reduction in aerosols and clouds and in ozone, the trend being  
21 caused by ozone changes which are approximately two thirds of the trend caused by aerosol  
22 and clouds changes.

23 As regards the 1950-2011 period, the most interesting series are San Sebastián, Madrid,  
24 Villalba, and the Iberian Peninsula series for the same reason as during the dimming period.  
25 All annual UVER series trends, except Madrid, are significant at 99% (95% for Murcia), this  
26 trend being  $25 \text{ Jm}^{-2}\text{dc}^{-1}$  ( $1.1\%\text{dc}^{-1}$ ) in the Iberian Peninsula, which indicates an increase of  $155$   
27  $\text{Jm}^{-2}$  (6.5%) in annual UVER irradiation over the last 62 years in the Iberian Peninsula. March  
28 presents positive and significant trends for the four most complete series, ranging from  $31 \text{ Jm}^{-2}\text{dc}^{-1}$   
29 (San Sebastián:  $2.2\%\text{dc}^{-1}$ ) to  $74 \text{ Jm}^{-2}\text{dc}^{-1}$  (Villalba:  $4.1\%\text{dc}^{-1}$ ). June and July exhibit the  
30 highest UVER trends, all of them proving significant except Madrid in July. The UVER trend  
31 in the Iberian Peninsula is  $83 \text{ Jm}^{-2}\text{dc}^{-1}$  ( $1.9\%\text{dc}^{-1}$ ) in June and  $47 \text{ Jm}^{-2}\text{dc}^{-1}$  ( $1.0\%\text{dc}^{-1}$ ) in July.  
32 As regards seasonal trends, all are significant in spring and summer except for spring in

1 Madrid. The trend in the Iberian Peninsula series is  $32 \text{ Jm}^{-2}\text{dc}^{-1}$  ( $1.2\%\text{dc}^{-1}$ ) in spring and  $54$   
2  $\text{Jm}^{-2}\text{dc}^{-1}$  ( $1.2\%\text{dc}^{-1}$ ) in summer. UVER trends in the 1950-2011 period are mainly caused by  
3 changes in TOC because these trends are similar to the obtained values of  $\text{TS}_{\text{O}_3}$ ,  $\text{TS}_{\text{ac}}$  being  
4 around zero. This result indicates that aerosol and clouds presence increasing during dimming  
5 and decreasing during brightening are well compensated over the 1950-2011 period.

#### 6 **4.1.4 UVER trends: Other periods**

7 In the previous section, UVER trends were calculated for three specific periods. Other  
8 authors, however, have calculated UVER trends for other periods in the literature. UVER  
9 trends were thus recalculated with the same UVER anomaly series but for other periods in  
10 this section in order to compare them with the results of other works.

11 Lindfors et al. (2003) reconstructed UVER irradiation at Sodankylä (Finland) between 1950  
12 and 1999 also using sunshine duration records, and reported two significant trends for this  
13 period:  $3.9\%\text{dc}^{-1}$  in March and  $-3.3\%\text{dc}^{-1}$  in July. Slightly higher significant trends were found  
14 in March for Madrid ( $5.3\%\text{dc}^{-1}$ ), Villalba ( $6.6\%\text{dc}^{-1}$ ), and the Iberian Peninsula ( $4.4\%\text{dc}^{-1}$ ) in  
15 the same period. These series do not present statistically significant trends in July for the  
16 1950-1999 period.

17 Bernhard et al. (2004) found no significant trend in the UVER irradiation measured in the  
18 South-Pole between 1991 and 2002. Positive and significant trends were obtained at Ciudad  
19 Real (February:  $19.4\%\text{dc}^{-1}$ ; June:  $16.1\%\text{dc}^{-1}$ ), Madrid (February:  $23.4\%\text{dc}^{-1}$ ), Murcia  
20 (February:  $30.6\%\text{dc}^{-1}$ ), and Tortosa (February:  $22.0\%\text{dc}^{-1}$ ) for the same period.

21 Josefsson (2006) analyzed the measured UVER at Norrköping (Sweden) between 1983 and  
22 2003, finding significant trends in UVER irradiation in spring ( $7.8\%\text{dc}^{-1}$ ), autumn ( $8.2\%\text{dc}^{-1}$ ),  
23 and in the annual series ( $5.2\%\text{dc}^{-1}$ ). Significant although lower trends were also detected in  
24 the same period in the series analyzed in this paper. The Iberian Peninsula series showed a  
25 significant trend of  $4.4\%\text{dc}^{-1}$  in spring and of  $2.7 \%\text{dc}^{-1}$  for the annual series.

26 Lindfors et al. (2007) reconstructed UVER irradiation using SW records from 1983 to 2005 in  
27 Bergen (Norway), Jokionen (Finland), Norrköping and Sodankylä, and reported a significant  
28 increase in annual UVER at Sodankylä ( $4.1\%\text{dc}^{-1}$ ). For the same period, trends in the annual  
29 UVER series at Cáceres, Murcia, and the Iberian Peninsula were similar and also significant,  
30 being  $3.2\%\text{dc}^{-1}$ ,  $2.7\%\text{dc}^{-1}$ , and  $2.7\%\text{dc}^{-1}$ , respectively.



1 den Outer et al. (2010) obtained UVER irradiation between 1980 and 2006 using different  
2 reconstruction models at eight European locations: Sodankylä, Jokionen, Norrköping,  
3 Potsdam (Germany), Lindenberg (Germany), Bilthoven (the Netherlands), Hradec Kralove  
4 (Czech Republic), and Thessaloniki (Greece). The annual UVER trends obtained by den  
5 Outer et al. (2010) range between  $2.8\%dc^{-1}$  and  $5.8\%dc^{-1}$ . The trends in the annual UVER  
6 series of this paper are all significant for the same period except for Murcia, and range  
7 between  $1.8\%dc^{-1}$  (Madrid) and  $5.3\%dc^{-1}$  (San Sebastián), with the Iberian Peninsula trend  
8 being  $3.2\%dc^{-1}$ . These results are similar to those obtained in literature.

9 Walker (2010) analyzed the trends of reconstructed UVER irradiation between 1981 and 2007  
10 at four Swiss locations: Davos, Payerne, Locarno, and Jungfrauoch, with the UVER  
11 irradiation trend proving significant in March and June for all four locations during this  
12 period. Spring and summer months present the highest number of significant trends in the  
13 UVER series of this work for the 1981-2007 period. Annual trends in Switzerland were  
14 similar to Spain (eight of the ten are significant) with values varying between  $2\%dc^{-1}$  and  
15  $4\%dc^{-1}$  from 1981 to 2007 in both countries, with  $3.0\%dc^{-1}$  being the trend in the annual  
16 Iberian Peninsula series.

17 Krzyscin et al. (2011) studied the UVER radiation observed at Belsk (Poland) between 1976  
18 and 2008, and found an annual trend of  $5.6\%dc^{-1}$ . In the same period, the trend in the annual  
19 Iberian Peninsula series was  $2.8\%dc^{-1}$ , half that of Belsk.

20 As regards UVER trends in the Iberian Peninsula obtained by other authors, three papers are  
21 well known. Bilbao et al. (2011) reconstructed UVER at Valladolid from 1991 to 2010 and  
22 found significant trends in summer ( $3.5\%dc^{-1}$ ) and autumn ( $4.1\%dc^{-1}$ ), similar to those  
23 obtained for the 1991-2010 period at Valladolid with the reconstructed series used in this  
24 paper:  $3.6\%dc^{-1}$  (summer) and  $5.9\%dc^{-1}$  (autumn). Antón et al. (2011a) reconstructed UVER  
25 irradiance at solar noon in summer from 1950 to 2000 at Badajoz (Spain) and Cáceres, and  
26 obtained a trend of  $4.9\%dc^{-1}$  for the 1979-2000 period at Cáceres. The significant UVER  
27 irradiation trend at Cáceres during the same period was  $5.2\%dc^{-1}$  using data from the present  
28 work, a similar value to that obtained by Antón et al. (2011a). This means that UVER  
29 irradiance trend at solar noon was similar to daily UVER irradiation trend at Cáceres. Finally,  
30 Ialongo et al. (2011) calculated UVER irradiation from 1979 to 2010 over the whole world  
31 using satellite images and found a UVER trend in the Iberian Peninsula of around  $2.5\%dc^{-1}$  in

1 March and October. The annual Iberian Peninsula series of the present work shows a similar  
2 trend ( $2.8\%dc^{-1}$ ) for the same period.

3 A comparison between the results obtained and those reported in the literature reveals that  
4 UVER changes in Europe have been similar, at least over the last few decades.

#### 5 **4.1.5 Effect of UVER uncertainty on trends**

6 The trends obtained were calculated without considering uncertainty in the UVER irradiation  
7 values, although uncertainty might influence the value and significance of trends. The effect  
8 of uncertainty on trends was studied following the method used by Román et al. (2014a, d):

9 For one specific series of UVER anomalies  $A$ , with  $N$  values  $A_i$ , and  $\sigma(A_i)$  being the  
10 uncertainty of the  $i$ -value of  $A$ , a normally distributed (centred on zero with a standard  
11 deviation of  $\sigma(A_i)$ ) random number ( $b_i$ ) is generated for each  $i$ -value. A normal distribution  
12 with a standard deviation of  $\sigma(A_i)$  is selected since it implies that the probability of finding a  
13 value  $A_i+b_i$  in the interval  $[A_i -\sigma(A_i), A_i +\sigma(A_i)]$  is about 68%, a probability that increases to  
14 95% when the interval is  $[A_i -2\sigma(A_i), A_i +2\sigma(A_i)]$ . Once the  $N$  values of  $b_i$  for all values of  $A$   
15 are obtained, a new synthetic series (SS) is formed as the sum of the original  $A$  series and the  
16 random numbers, the  $i$ -value of the SS series being equal to  $A_i+b_i$ . The SS series is physically  
17 valid since it is inside the uncertainty of the  $A$  series.

18 10,000 synthetic SS series were randomly obtained for each series analyzed in the previous  
19 section following the methodology described, and their trends and significance were  
20 calculated. The percentage of the 10,000 series whose trend is statistically significant at 95%  
21 ( $P(p<0.05)$ ), and at 99% ( $P(p<0.01)$ ), was calculated. Only the series with a value of  
22  $P(p<0.05)$  and  $P(p<0.01)$  above 95% and 99% were considered statistically significant at 95%  
23 and 99%, respectively. 55% (65 out of 119, considering the 10 locations and the 12 monthly +  
24 4 seasonal + 1 annual) of the significant trends (in 1950-2011, 1950-1984, and 1985-2011  
25 periods) with at least 95% confidence are considered significant (95% confidence) using the  
26 criterion based on uncertainties. All series not considered significant in the previous section  
27 are not significant with the uncertainty-based criterion.

28 The  $P(p<0.05)$  and  $P(p<0.01)$  values of the seasonal and annual UVER series considered  
29 statistically significant with at least 95% confidence taking into account the uncertainty are  
30 shown in Table 4. High  $P(p<0.05)$  values do not imply high  $P(p<0.01)$  values. The median  
31 and standard deviation of the 10,000 values of TS calculated from all synthetic series are also

1 included in Table 4. These trends are similar to the trends in Table 3, the differences between  
2 them being below  $5 \text{ Jm}^{-2}\text{dc}^{-1}$  ( $0.1\%\text{dc}^{-1}$ ) in most cases, although this difference reaches  $18 \text{ Jm}^{-2}\text{dc}^{-1}$  ( $0.4\%\text{dc}^{-1}$ ) for Ciudad Real in summer in the 1985-2011 period. These differences are  
3 always below the standard deviation of the trend given in Table 4 (except for Ciudad Real in  
4 summer in the 1985-2011 period).

## 6 4.2 UVER irradiation over open body

### 7 4.2.1 Temperature and open body fraction

8 Monthly averages of daily mean temperature, daily effective temperature, daily open body  
9 fraction, and all their monthly anomalies were calculated using the same method as in the  
10 UVER case. Seasonal and annual anomalies were also calculated. Fig. 6 shows the evolution  
11 of the annual  $T_m$  anomalies for the averaged Iberian Peninsula series. **The behaviour of  $t_{\text{eff}}$ ,  
12 and S (not shown) is similar since S is directly connected with  $t_{\text{eff}}$ , and  $t_{\text{eff}}$  with  $T_m$  (Sect. 2).**  
13  $T_m$  (and  $t_{\text{eff}}$  and S) fell between the 1950s and the 1970s, and began to increase in the 1970s.  
14 Similar results were obtained for the whole Northern Hemisphere (Hansen and Lebedeff,  
15 1987; Wild, 2012). The increase in mean temperature is usually attributed to an increase in  
16 greenhouse gases ( $\text{CO}_2$ ,  $\text{CH}_4$ , etc.), sparking the well known “global warming” phenomenon.

17  $T_m$  presents significant trends in the 1950-2011 period for the Iberian Peninsula series,  
18 ranging from  $0.17^\circ\text{Cdc}^{-1}$  in autumn to  $0.31^\circ\text{Cdc}^{-1}$  in summer. A significant and negative trend  
19 was observed in  $T_m$  of  $-0.44^\circ\text{Cdc}^{-1}$  in the Iberian Peninsula in spring for the dimming period.  
20 This might be caused by the decrease in  $T_m$  up to the 1970s observed in Fig. 6. The mentioned  
21 decrease was caused by the dimming phenomenon, since the reduction in SW radiation (due  
22 to aerosol increase) cooled the Earth while the increase in greenhouse gases warmed it, the  
23 dimming effect proving stronger up to the 1970s (IPCC, 2007). The decrease between 1950  
24 and 1970 was not found in the Southern Hemisphere (where aerosol emissions were one order  
25 of magnitude smaller than in the Northern Hemisphere), supporting the hypothesis that  
26 increased aerosol load cooled the Earth more strongly than greenhouse gas increases warmed  
27 it up to 1970 (Wild, 2012). On the other hand, increased SW irradiation (caused by aerosol  
28 reduction) and greenhouse gases both warmed the Earth during the brightening period. In fact,  
29 the Iberian Peninsula series of  $T_m$  presented positive and significant trends in spring ( $0.55$   
30  $^\circ\text{Cdc}^{-1}$ ) and summer ( $0.36 \text{ }^\circ\text{Cdc}^{-1}$ ) for the 1985-2011 period, which are higher than those  
31 obtained for the 1950-2011 period. The last decade in Fig. 6 shows a reduction in temperature

1 increase, which might be linked to a new increase in sulphur aerosol particles worldwide due  
2 to emissions in Asia after the year 2000 (Streets et al., 2009). This aerosol increase was  
3 observed by Chin et al. (2013), and might be sparking a new dimming phenomenon, which  
4 might have been occurring in China and India since 2000 (Wild et al., 2009; Wild, 2012).

5 The increase in mean temperature leads to an increase in effective temperature and, hence, in  
6 the open body fraction. This increase means that the surface area of naked human body  
7 exposed to the sun has increased over the last few decades, mainly due to an increase in mean  
8 temperature caused by increased greenhouse gases and, for the brightening period, also by  
9 aerosol (and also clouds due to the indirect effect) reduction.

#### 10 **4.2.2 UVER over open body evolution**

11 UVER irradiation quantifies the toxicity of solar radiation over human skin. However, if the  
12 human body is totally covered by clothes or anything else, the skin will not be affected by sun  
13 exposure even for high UVER irradiation values. Therefore, in order to find a new variable  
14 which quantifies the UVER dose received by human skin, the UVER over open body  
15 ( $UVER_{ob}$ ) is defined as the UVER radiation multiplied by the open body fraction.  **$UVER_{ob}$**   
16 **irradiation, measured in  $Jm^{-2}$  per open body unit, physically means the daily UVER irradiation**  
17 **received over the naked skin of a human who is exposed to sun the whole day. The open body**  
18 **fraction is usually multiplied by the UV radiation weighted by the vitamin D synthesis action**  
19 **spectrum (e.g., Chubarova and Zhdanova, 2013), but not by UVER radiation. The damage of**  
20 **UV over human skin is cumulative (WHO, 2002), and  $UVER_{ob}$  can be used to evidences how**  
21 **much portion of skin is damaged or how much bigger is the redness skin after an**  
22 **overexposure to sun.**

23 **In this work, the daily UVER irradiation of each series was multiplied by the daily open body**  
24 **fraction, obtaining the daily  $UVER_{ob}$  irradiation.** The  $UVER_{ob}$  irradiation series obtained were  
25 monthly averaged, and monthly, seasonal, and annual anomalies were then calculated  
26 following the same process as in Sect. 4.1. Figure 7 shows the annual  $UVER_{ob}$  evolution for  
27 the ten series. The expected results for  $UVER_{ob}$  should be different to the UVER analysis due  
28 to the changes in S. However, annual  $UVER_{ob}$  evolution is similar to that of UVER in Fig. 4.  
29 The increase in  $UVER_{ob}$  during the brightening period seems larger than for UVER, probably  
30 due to the increase in the open body fraction caused by  $T_m$  variations (Fig. 6). The reduction

1 in  $UVER_{ob}$  should be bigger than in  $UVER$  due to the reduction in effective temperature up to  
2 the 1970s, although this cannot be seen in Fig. 7.

### 3 **4.2.3 $UVER_{ob}$ trends**

4 In order to quantify the results observed in Fig. 7, the trends and their significance of all  
5 available  $UVER_{ob}$  series were calculated in the same way as in the  $UVER$  section. Figure 8  
6 shows the  $UVER_{ob}$  trends (and their significance and 95CI) for all monthly, seasonal, and  
7 annual series for all locations at three periods. In addition, the statistically significant seasonal  
8 and annual trends are shown in Table 5 for the three periods.

9 As regards the 1950-1984 period,  $UVER_{ob}$  irradiation shows only a few more significant  
10 trends than the  $UVER$  case. However, the Iberian Peninsula series shows a statistically  
11 significant (99% confidence) trend of  $-4.3\%dc^{-1}$  in spring, and a statistically significant (95%  
12 confidence) trend of  $-1.5\%dc^{-1}$  for the annual series. This significant reduction in spring  
13 could be related to the significant decrease observed in  $T_m$  ( $-0.44^{\circ}Cdc^{-1}$ ) during the same  
14 period.

15 In the brightening period, all annual  $UVER_{ob}$  series, except A Coruña and Madrid, show  
16 significant trends, ranging from  $2.9\%dc^{-1}$  (Villalba) to  $5.0\%dc^{-1}$  (San Sebastián). There are  
17 more significant and higher trends, especially with 99% confidence and in summer-spring  
18 months, in the  $UVER_{ob}$  series than in  $UVER$  for the 1985-2011 period, which is due to the  
19 increase in  $T_m$ , and therefore in  $S$ , in this period. The difference between the  $UVER_{ob}$  trend  
20 and the  $UVER$  trend accounts for the part of the  $UVER_{ob}$  trend caused by open body fraction  
21 changes, and therefore by effective temperature changes.  $UVER$  in the Iberian Peninsula  
22 increased by  $2.5\%dc^{-1}$ (summer) and  $2.1\%dc^{-1}$  (annual) during brightening, the same trends  
23 being  $3.6\%dc^{-1}$ (summer) and  $3.8\%dc^{-1}$  (annual) in the  $UVER_{ob}$  case. This implies that the  
24 effective temperature changes are responsible for more than  $1\%dc^{-1}$  (~30% and ~45% of the  
25 total trend) of the changes observed in  $UVER_{ob}$  between 1985 and 2011 in the Iberian  
26 Peninsula. The portion of each  $UVER_{ob}$  trend caused by ozone, aerosol and clouds, and  
27 effective temperature can be calculated taking into account the  $TS_{o_3}$  and  $TS_{ac}$  values in Table  
28 3. 28.9%, 39.1%, and 32.0% of the  $UVER_{ob}$  trend in the Iberian Peninsula in summer  
29 ( $3.6\%dc^{-1}$ ) were caused by changes in ozone, aerosol and clouds, and effective temperature,  
30 respectively. These percentages were 20.7%, 35.1%, and 44.2% for the same trend in the  
31  $UVER_{ob}$  annual series ( $3.8\%dc^{-1}$ ).

1 As regards the 1950-2011 period, all annual and summer  $UVER_{ob}$  trends were significant with  
2 99% confidence. The annual  $UVER_{ob}$  trends in this period were  $2.3\%dc^{-1}$ ,  $1.9\%dc^{-1}$ ,  $1.8\%dc^{-1}$   
3 and  $2.0\%dc^{-1}$ , for San Sebastián, Madrid, Villalba, and the Iberian Peninsula, respectively. In  
4 fact the annual  $UVER_{ob}$  increased by a total of 12.5% between 1950 and 2011 in the Iberian  
5 Peninsula. Higher and more statistically significant trends appear in  $UVER_{ob}$  series than in  
6  $UVER$  for the 1950-2011 period, especially in spring and summer months, as Fig. 8 reveals.  
7 This is caused by the rise in the open body fraction over the last six decades as a result of  
8 effective temperature increase.  $UVER$  changes in this period were mainly caused by ozone  
9 changes, the  $UVER_{ob}$  trends thus being mainly caused by ozone and effective temperature  
10 changes. The  $UVER_{ob}$  trend in summer for the Iberian Peninsula was  $2.4\%dc^{-1}$ ,  $1.1\%dc^{-1}$   
11 being caused by changes in effective temperature. Moreover, half of the annual Iberian  
12 Peninsula trend was caused by effective temperature. In the 1950-2011 period, 45.4%, 7.8%,  
13 and 46.8% of the  $UVER_{ob}$  trend in the Iberian Peninsula in summer ( $2.4\%dc^{-1}$ ) was caused by  
14 changes in ozone, aerosol and clouds, and effective temperature, respectively. These  
15 percentages were 50.8%, 1.2%, and 48.0% for the same trend in the  $UVER_{ob}$  annual series  
16 ( $2.0\%dc^{-1}$ ). These results reveal that changes in  $UVER$  on the open body over the last six  
17 decades have mainly been caused by ozone and temperature changes in a similar proportion,  
18 with the influence of aerosol and clouds changes on  $UVER_{ob}$  proving to be negligible.

19 The same results were obtained considering the effective temperature equal to the mean  
20 temperature in order to calculate the open body fraction with Eq. (3). Hence,  $UVER_{ob}$  changes  
21 caused by effective temperature can be considered to be changes caused by the mean  
22 temperature, disregarding the influence of relative humidity or wind speed changes.

23

## 24 **5 Factors not taken into account**

25 The results of this paper were obtained using reconstructed data series by models. However,  
26 the paper is not without certain limitations. Changes in aerosol optical depth, surface albedo  
27 or water vapour column were not considered, these variables being used in the radiative  
28 transfer model as monthly climatology.

29 The lack of AOD data earlier 2000 led to use a climatological table which does not contain  
30 the aerosol changes in the 1950-2011 period. However the aerosol effect is included the SW  
31 and F measurements (like clouds) and, as a first approximation, the reconstruction models

1 transfer this effect to the UVER radiation. This approximation is not valid for the case of  
2 water vapour because it affects SW and F but not UVER.

3 If the water vapour column had increased, cloudless SW irradiation would have decreased  
4 and, therefore, reconstructed UVER should be higher. Daily water vapour column trends were  
5 calculated between 1957 and 2002 in the Iberian Peninsula using the daily ERA-40 data  
6 (Uppala et al., 2005; Lindfors et al., 2007). These trends (not shown) indicate a slight water  
7 vapour decrease in recent decades, which did not always prove significant, but which might  
8 contribute to reducing the UVER trends obtained.

9 Trends in surface albedo at 360 nm (Sect. 2.2) from 1958 to 2002 were calculated (not  
10 shown), revealing that, apart from a slight decrease in winter months, surface albedo has  
11 suffered no significant changes in recent decades. This result indicates that the UVER trend  
12 obtained in winter might be slightly lower due to changes in albedo, but should not affect the  
13 remaining months.

14 A further factor to take into account should be the uncertainty of the data used (caused in part  
15 by the monthly variability of the radiative transfer inputs), since certain trends cannot be  
16 considered significant when uncertainty is taken into account, as can be seen in Sect. 4.1.5.  
17 Moreover, the averaged Iberian Peninsula anomaly series was calculated using nine locations,  
18 with only four or five locations having data available for the years prior to 1970. This number  
19 of locations might not be sufficient to obtain a representative averaged result for the Iberian  
20 Peninsula. However, by way of an initial approximation, the number of locations was  
21 considered representative since when using the same locations, Román et al. (2014a) obtained  
22 similar results in SW irradiation to Sánchez-Lorenzo et al. (2013a), who used more locations  
23 to obtain an averaged Iberian Peninsula series.

24 Finally, as regards UVER irradiation over open body, it was considered that a rise in  
25 temperature increases the surface area of naked human body exposed to the sun. However,  
26 increased temperatures might lead to the opposite effect since when temperatures increase,  
27 humans do not remove more clothing but decide to protect themselves from the sun (e.g., by  
28 staying at home), thereby preventing the impact of solar radiation on the body. A further  
29 factor not considered is the effect of the growing number of buildings in urban locations,  
30 since such an increase might lead to a rise in the number of shady areas, where UVER  
31 irradiation is less. Finally, as regards changes in UVER irradiation received by the human  
32 body, two important factors were not taken into account: firstly, the use of creams and

1 sunscreen products whose use would curb damage to human skin; and secondly the opposite  
2 effect, the fashion for getting a tan, which leads to greater exposure to the sun and further  
3 damage to the skin, causing diseases like tanorexia (tanning addiction), in which the patient  
4 has an obsessive need to achieve a darker skin tone.

5 All these factors might impact the results obtained vis-à-vis changes in the real skin damage  
6 to people caused by solar radiation in the Iberian Peninsula.

7

## 8 **6 Conclusions**

9 UVER irradiation in the Iberian Peninsula increased by  $2.1\%dc^{-1}$  (annual) and  $2.5\%dc^{-1}$   
10 (summer) for the 1985-2011 period, and  $1.1\%dc^{-1}$  (annual) and  $1.3\%dc^{-1}$  (summer) for the  
11 1950-2011 period. The amount of ozone in the atmosphere is returning to pre-1980 levels due  
12 to the reduction in halogen gases subsequent to the Montreal Protocol. Said reduction  
13 supports the belief that increased UVER radiation over the past 27 years has in large part been  
14 due to a reduction in the release of aerosols into the atmosphere, also reducing the cloud  
15 presence (brightening). However, increased UVER was mainly caused by ozone depletion  
16 during the 1950-2011 period. A significant UVER trend can become non-significant when  
17 uncertainty in the reconstructed data is taken into account.

18 The major changes in UVER radiation on naked human skin (open body) are due to: changes  
19 in ozone (caused by changes in halogen gas emissions), changes in aerosols and clouds  
20 (dimming and brightening), and changes in temperature (global warming). The annual Iberian  
21 Peninsula UVER<sub>ob</sub> series evidenced a significant annual increase of  $3.8\%dc^{-1}$  and a significant  
22 seasonal increase of  $3.6\%dc^{-1}$  in summer for the 1985-2011 period. These trends are caused  
23 mainly by temperature and aerosol and clouds changes. As regards the 1950-2011 period, the  
24 annual ( $2.0\%dc^{-1}$ ) and summer ( $2.4\%dc^{-1}$ ) UVER<sub>ob</sub> trends in the Iberian Peninsula were  
25 mainly caused by ozone and temperature changes in a similar proportion.

26 In future, an increase in the amount of aerosols in the atmosphere would spark lower UVER  
27 radiation and temperature levels, leading to a reduction in UVER irradiation over the open  
28 body in two ways. However, increased air pollution is totally inadmissible, since this would  
29 lead to an increase in cardio-respiratory and other diseases, and might have a devastating  
30 effect on the climate, for instance by causing severe droughts. Once the increase in  
31 anthropogenic aerosols in the atmosphere has been discarded, and bearing in mind that ozone



1 levels have continued to rise since the Montreal protocol, UVER irradiation over the open  
2 body should be reduced by lowering the temperature (in other words, by avoiding global  
3 warming). Reducing anthropogenic aerosols in the atmosphere leads to an increase in  
4 temperature. Hence, the amount of aerosols and greenhouse gas emissions into the  
5 atmosphere must be cut, whilst preventing increased temperatures caused by the greenhouse  
6 effect and a new brightening. Therefore, reducing air pollution and cutting greenhouse gas  
7 emissions might not only reduce global warming, with the possible benefits this would entail,  
8 but would also restrict the amount of harmful solar radiation received by human skin. Finally,  
9 human beings must be responsible for preventing diseases related to sun exposure by avoiding  
10 contact with the sun around midday and taking the necessary precautions (sunscreen creams,  
11 sunshades, etc.) in order to enjoy healthy sun exposure and the beneficial effects of solar  
12 radiation.

### 13 **Acknowledgements**

14 The authors gratefully acknowledge the financial support extended by the Spanish Ministry of  
15 Science and Innovation for project CGL2011-25363. The authors also thank the staff at the  
16 AEMet for the data used and for their effort in establishing and maintaining the stations. The  
17 authors gratefully thank the OMI, TOMS, GOME, GOME-2, MODIS, and MISR teams for  
18 the satellite data used in this study, as well as the staff of the COST-726 project for the  
19 reconstructed ozone data. The NASA GES DISC and the AVDC are also acknowledged for  
20 the GIOVANNI application and the satellite overpass files. Roberto Román would like to  
21 thank the University of Valladolid for its support through the PIF-UVa grant.

22

23

24

25

26

27

28

29

30

## 1 **References**

- 2 Acker, J. G. and Leptoukh, G.: Online Analysis Enhances Use of NASA Earth Science Data,  
3 Eos, Trans. AGU, 88, 2 14-17, 2007.
- 4 Alexandersson, H. and Moberg, A.: Homogenization of Swedish temperature data. Part I:  
5 Homogeneity test for linear trends, Int. J. Climatol., 17, 25–34, 1997.
- 6 Anderson, G., Clough, S., Kneizys, F., Chetwynd, J., and Shettle, E.: AFGL atmospheric  
7 constituent profiles (0-120 km), Tech. Rep. AFGL-TR-86-0110, Air Force Geophys. Lab.,  
8 Hanscom Air Force Base, Bedford, Mass., 1986.
- 9 Antón, M., Serrano, A., Cancillo, M. L., García, J. A., and Madronich, S.: Application of an  
10 analytical formula for UV Index reconstructions for two locations in Southwestern Spain,  
11 Tellus, 63B, 1052–1058, 2011a.
- 12 **Antón, M., Serrano, A., Cancillo, M. L., García, J.A., and Madronich, S.: Empirical**  
13 **evaluation of a simple analytical formula for the ultraviolet index, Photochem. Photobiol., 87,**  
14 **478–482, 2011b.**
- 15 Bernhard, G., Booth, C. R., and Ebrahimian, J. C.: Version 2 data of the National Science  
16 Foundation’s Ultraviolet Radiation Monitoring Network: South Pole, J. Geophys. Res., 109,  
17 D21207, 2004.
- 18 Bilbao, J., Román, R., de Miguel, A., and Mateos, D.: Long-term solar erythemal UV  
19 irradiance data reconstruction in Spain using a semiempirical method, J. Geophys. Res., 116,  
20 D22211, 2011.
- 21 **Bodeker, G. E. and McKenzie, R.L.: An algorithm for inferring surface UV irradiance**  
22 **including cloud effects, J. Appl. Meteorol., 35, 10, 1860–1877, 1996.**
- 23 Buras, R., Dowling, T., and Emde, C.: New secondary-scattering correction in DISORT with  
24 increased efficiency for forward scattering, J. Quant. Spectrosc. Ra., 112, 2028–2034,  
25 doi:10.1016/j.jqsrt.2011.03.019, 2011.
- 26 **Calbó, J., Pagès, D., and González, J. A.: Empirical studies of cloud effects on UV radiation:**  
27 **A review, Rev. Geophys., 43, 2, 1-28, 2005.**
- 28 Chin, M., et al.: Multi-decadal variations of atmospheric aerosols from 1980 to 2009: sources  
29 and regional trends, Atmos. Chem. Phys. Discuss., 13, 19751–19835, 2013.

- 1 Chubarova, N. and Zhdanova, Y.: Ultraviolet resources over Northern Eurasia, *J. Photoch.*  
2 *Photobio. B.*, 127, 38-51, 2013.
- 3 de Miguel, A., Bilbao, J., Román, R., and Mateos, D.: Measurements and attenuation of  
4 erythemal radiation in Central Spain, *Int. J. Climatol.*, 32, 929–940, 2012.
- 5 den Outer, P. N., Slaper, H., Matthijsen, J., Reinen, H. A. J. M., and Tax, R.: Variability of  
6 ground-level ultraviolet: Model and measurement, *Radiat. Prot. Dosim.*, 91, 105-110, 2000.
- 7 den Outer, P. N., Slaper, H., and Tax, R. B.: UV radiation in the Netherlands: Assessing long-  
8 term variability and trends in relation to ozone and clouds, *J. Geophys. Res.*, 110, D02203,  
9 2005.
- 10 den Outer, P. N., Slaper, H., Kaurola, J., Lindfors, A., Kazantzidis, A., Bais, A. F., Feister, U.,  
11 Junk, J., Janouch, M., and Josefsson, W.: Reconstructing of erythemal ultraviolet radiation  
12 levels in Europe for the past 4 decades, *J. Geophys. Res.*, 115, D10102, 2010.
- 13 Gilbert, R. O.: Statistical methods for environmental pollution monitoring, Van Nostrand  
14 Company, Hoboken, N. J., 320 pp, 1987.
- 15 Hakuba, M. Z., Sánchez-Lorenzo, A., Folini, D., and Wild, M.: Testing the homogeneity of  
16 short-term surface solar radiation series in Europe, *AIP Conf. Proc.*, 1531, 700, 2013.
- 17 Hansen, J. and Lebedeff, S.: Global Trends of Measured Surface Air Temperature, *J.*  
18 *Geophys. Res.*, 92, 13345-13372, 1987.
- 19 Hülsen, G. and Gröbner, J.: Characterization and calibration of ultraviolet broadband  
20 radiometers measuring erythemal weighted irradiance, *Appl. Opt.*, 26, 23, 5877-5886, 2007.
- 21 Ialongo, I., Arola, A., Kujanpää, J., and Tamminen, J.: Use of satellite erythemal UV products  
22 in analysing the global UV changes, *Atmos. Chem. Phys.*, 11, 9649–9658, 2011.
- 23 IPCC (Intergovernmental Panel on Climate Change): IPCC Fourth Assessment Reports  
24 (AR4): Working Group I Report: Climate Change 2007, The Physical Basis, WMO/UNEP  
25 Report, 2007.
- 26 Iqbal, M.: An introduction to solar radiation, Academic Press, 0-12-373750-8, 1983.
- 27 Josefsson, W.: UV-radiation 1983-2003 measured at Norrköping, Sweden, *Theor. Appl.*  
28 *Climatol.*, 83, 59-76, 2006.

1 **Kaurola, J., Taalas, P., Koskela, T., Borkowski, J., and Josefsson, W.: Long-term variations of**  
2 **UV-B doses at three stations in northern Europe, *J. Geophys. Res.*, 105, D16, 20813–20820,**  
3 **2000.**

4 Krzyscin, J. W.: Statistical reconstruction of daily total ozone over Europe 1950 to 2004, *J.*  
5 *Geophys. Res.*, 113, D07112, 2008.

6 Krzyscin, J. W., Sobolewski, P. S., Jarosławski, J., Podgórski, J., and Rajewska-Wiech, B.:  
7 Erythemal UV observations at Belsk, Poland, in the period 1976–2008: data homogenization,  
8 climatology, and trends, *Acta Geophys.*, 59, 155–182, 2011.

9 Kurucz, R.: Synthetic infrared spectra, Proceedings of the 154th Symposium of the  
10 International Astronomical Union (IAU), 1992.

11 Kylling, A., Stamnes, K., and Tsay, S. C.: A reliable and efficient two-stream algorithm for  
12 spherical radiative transfer: Documentation of accuracy in realistic layered media, *J. Atmos.*  
13 *Chem*, 21, 115-150, 1995.

14 Lindfors, A., Arola, A., Kaurola, J., Arola, A., Taalas, P., and Svenoe, T.: Long-term  
15 erythemal UV doses at Sodankylä estimated using total ozone, sunshine duration, and snow  
16 depth, *J. Geophys. Res.*, 108 (D16), 4518, 2003.

17 Lindfors, A., Kaurola, J., Arola, A., Koskela, T., Lakkala, K., Josefson, W., Olseth, J. A., and  
18 Johnsen, B.: A method for reconstruction of past UV radiation based on radiative transfer  
19 modeling: Applied to four stations in northern Europe, *J. Geophys. Res.*, 112, D23201, 2007.

20 **Matthijsen, J., Slaper, H., Reinen, H. A. J. M., and Velders, G. J. M.; Reduction of solar UV**  
21 **by clouds: A comparison between satellite-derived cloud effects and ground-based radiation**  
22 **measurements, *J. Geophys. Res.*, 105, D4, 5069-5080, 2000.**

23 Mayer, B. and Kylling, A.: Technical note: The libRadtran software package for radiative  
24 transfer calculations – description and examples of use, *Atmos. Chem. Phys.*, 5, 1855–1877,  
25 2005.

26 McKinlay, A. F. and Diffey, B. L.: A reference action spectrum for ultraviolet induced  
27 erythema in human skin, Commission Internationale de l' Eclairage (CIE), 6, 17–22, 1987.

28 Moreta J. R., García, R., Martín, L., Montero, J., San Atanasio, J. M., Hernández, J. L., Díaz,  
29 A., Vicente, R., C.R.N., and López, M.: AEMet contribution to the WMO/GAW programme,  
30 GAW 2013 Symposium, WMO Secretariat, Geneva, 2013.

1 Peter, T.: Microphysics and heterogeneous chemistry of polar stratospheric clouds, *Annu.*  
2 *Rev. Phys. Chem.*, 48, 785–822, 1997.

3 **Piedehierro, A. A., Antón, M., Cazorla, A., Alados-Arboledas, L., Olmo, F. J.: Evaluation of**  
4 **enhancement events of total solar irradiance during cloudy conditions at Granada**  
5 **(Southeastern Spain), *Atmos. Res.*, 135:136, 1-7, 2014.**

6 Ricchiazzi, P., Yang, S., Gautier, C., and Sowle, D.: SBDART: A research and Teaching  
7 software tool for plane-parallel radiative transfer in the Earth's atmosphere, *Bulletin of the*  
8 *American Meteorological Society*, 79, 2101–2114, 1998.

9 Rieder, H. E., Holawe, F., Simic, S., Blumthaler, M., Krzyscin, J. W., Wagner, J. E.,  
10 Schmalwieser, A. W., and Weihs, P.: Reconstruction of erythemal UV-doses for two stations  
11 in Austria: a comparison between alpine and urban regions, *Atmos. Chem. Phys.*, 8, 6309–  
12 6323, 2008.

13 Rieder, H. E., Frossard, L., Ribatet, M., Staehelin, J., Maeder, J. A., Di Rocco, S., Davison, A.  
14 C., Peter, T., Weihs, P., and Holawe, F.: On the relationship between total ozone and  
15 atmospheric dynamics and chemistry at mid-latitudes – Part 2: The effects of the El  
16 Niño/Southern Oscillation, volcanic eruptions and contributions of atmospheric dynamics and  
17 chemistry to long-term total ozone changes, *Atmos. Chem. Phys.*, 13, 165–179, 2013.

18 **Román, R.: Reconstrucción y análisis de la radiación ultravioleta eritemática en la Península**  
19 **Ibérica desde 1950, PhD Thesis, Dep. of Appl. Phys., Univ. of Valladolid, Valladolid, Spain,**  
20 **2014.**

21

22 Román, R., Bilbao, J., and de Miguel, A.: Reconstruction of six decades of daily total solar  
23 shortwave irradiation in the Iberian Peninsula using sunshine duration records, *Atmos.*  
24 *Environ.*, ATMENV-D-14-00791R1, under review, 2014a.

25 Román, R., Bilbao, J., and de Miguel, A.: Solar radiation simulations in the Iberian Peninsula:  
26 Accuracy and sensitivity to uncertainties in inputs of a radiative transfer model, *J. Quant.*  
27 *Spectrosc. Ra.*, 145, 95–109, doi: [10.1016/j.jqsrt.2014.04.028](https://doi.org/10.1016/j.jqsrt.2014.04.028), 2014b.

28 Román, R., Bilbao, J., and de Miguel, A.: Uncertainty and variability in satellite-based water  
29 vapor column, aerosol optical depth and Angström Exponent, and its effect on radiative  
30 transfer simulations in the Iberian Peninsula, *Atmos. Environ.*, 89, 556-569, 2014c.

1 Román, R., Bilbao, J., and de Miguel, A.: Uncertainty of different atmospheric ozone  
2 retrievals and its effect on temporal trends and on a radiative transfer simulations in the  
3 Iberian Peninsula, *J. Geophys. Res. Atmos.*, 119, published online,  
4 doi:10.1002/2013JD021260., 2014d.

5 **Sabburg, J. and Parisi, A. V.: Spectral dependency of cloud enhanced UV irradiance, *Atmos.*  
6 *Res.* 81, 206–214, 2006.**

7 **Sabburg, J., and Calbó, J.: Five years of cloud enhanced surface UV radiation measurements  
8 at two sites (in the Northern and Southern Hemispheres), *Atmos. Res.*, 93, 4, 902-912, 2009.**

9 Sánchez-Lorenzo, A., Brunetti, M., Calbó, J., and Martin-Vide, J.: Recent spatial and  
10 temporal variability and trends of sunshine duration over the Iberian Peninsula from a  
11 homogenized data set, *J. Geophys. Res.*, 112, D20115, 2007.

12 Sánchez-Lorenzo, A., Calbó, J., and Wild, M.: Global and diffuse solar radiation in Spain:  
13 Building a homogeneous dataset and assessing their trends, *Global Planet. Change*, 100, 343-  
14 352, 2013a.

15 Sánchez-Lorenzo, A., Wild, M., Guijarro, J. A., Brunetti, M., Bartok, B., Mystakidis, S.,  
16 Hakuba, M., and Müller, G.: Reassessment and update of the trends in the surface solar  
17 radiation over Europe by means of homogenized series from the GEBA, European  
18 Geophysical Union (EGU) General Assembly 2013, 2013b.

19 Sánchez-Lorenzo, A., Wild, M., and Trentmann, J.: Validation and stability assessment of the  
20 monthly mean CM SAF surface solar radiation dataset over Europe against a homogenized  
21 surface dataset (1983-2005), *Rem. Sens. Env.*, 134 355-366, 2013c.

22 Schaaf, C. B., et al.: First Operational BRDF, Albedo and Nadir Reflectance Products from  
23 MODIS, *Remote Sens. Environ.*, 83, 135-148, 2002.

24 Schwander, H., Mayer, B., Ruggaber, A., Albold, A., Seckmeyer G., and Koepke, P.: Method  
25 to determine snow albedo values in the UV for radiative transfer modelling, *Appl. Optics*, 38,  
26 18, 3869–3875, 1999.

27 Shettle, E.: Models of aerosols, clouds and precipitation for atmospheric propagation studies,  
28 Atmospheric propagation in the uv, visible, ir and mm-region and related system aspects, 454  
29 in AGARD Conference Proceedings, 1989.

- 1 Solomon, S.: Stratospheric ozone depletion: a review of concepts and history, *Rev. Geophys.*,  
2 37, 275–316, 1999.
- 3 Stanhill, G. and Cohen, S.: Global dimming: A review of the evidence for a widespread and  
4 significant reduction in global radiation, *Agric. For. Meteorol.*, 107, 255-278, 2001.
- 5 Steadman, R.G.: The assessment of sultriness. Part I: A temperature-humidity index based on  
6 human physiology and clothing science, *J. Appl. Meteor.*, 18, 861-873, 1979.
- 7 Streets, D. G., et al.: Anthropogenic and natural contributions to regional trends in aerosol  
8 optical depth, 1980–2006, *J. Geophys. Res.*, 114, D00D18, 2009.
- 9 Tanskanen, A.: Lambertian Surface Albedo Climatology at 360 nm from TOMS Data Using  
10 Moving Time-Window Technique, *Proceedings of the XX Quadrennial Ozone Symposium*,  
11 2004.
- 12 UNEP (United Nations Environment Programme): UNEP assessment reports: Environmental  
13 effects of ozone depletion and its interactions with climate change: 2002 assessment,  
14 *Photochem. Photobiol. Sci.*, 2, 1-72, 2003.
- 15 Uppala, S., et al.: The ERA-40 re-analysis, *Q. J. R. Meteorol. Soc.*, 131, 2961-3012, 2005.
- 16 Van Hoosier, M. E., Bartoe, J.-D. F., Brueckner, G. E., and Prinz, D. K.: Absolute solar  
17 spectral irradiance 120 nm - 400 nm (Results from the Solar Ultraviolet Spectral Irradiance  
18 Monitor - SUSIM- Experiment on board Spacelab 2), *Astro. Lett. and Communications*, 27,  
19 163-168, 1988.
- 20 Vicente-Serrano, S. M., Azorin-Molina, C., Sánchez-Lorenzo, A., Morán-Tejada, E.,  
21 Lorenzo-Lacruz, J., Revuelto, J., López-Moreno, J. I., and Espejo, F.: Temporal evolution of  
22 surface humidity in Spain: recent trends and possible physical mechanisms, *Clim. Dyn.*,  
23 published online, doi:10.1007/s00382-013-1885-7, 2013.
- 24 Vilaplana, J. M., Cachorro, V. E., Sorribas, M., Luccini, E., de Frutos, A. M., Berjón, A., and  
25 de la Morena, B.: Modified calibration procedures for a yankee environmental system UVB-1  
26 biometer based on spectral measurements with a brewer spectrophotometer, *Photochem.*  
27 *Photobiol.*, 82, 508–514, 2009.
- 28 Walker, D.: Cloud effects on erythemal UV radiation in a complex topography, PhD Thesis,  
29 *Veröffentlichungen der MeteoSchweiz*, 86, 106 p, ISSN: 1422-1381, 2010.

1 Webb, A. R.: Who, what, where and when-influences on cutaneous vitamin D synthesis, Prog.  
2 Biophys. Mol. Biol., 92, 17–25, 2006.

3 Webb, A., Gröbner, J., and Blumthaler, M.: A Practical Guide to Operating Broadband  
4 Instruments Measuring Erythemally Weighted Irradiance, COST726, 22595, 92-898-0032-1,  
5 2006.

6 WHO (World Health Organization): Protection against exposure to ultraviolet radiation,  
7 Technical Report WHO/EHG 17, 1995.

8 WHO (World Health Organization): Global Solar UV Index: A Practical Guide, 28 pp., ISBN  
9 92-4-159007-6, Geneva, Switzerland, 2002.

10 Wijngaard, J. B., Klein-Tank, A. M. G., and Können, G. P.: Homogeneity of 20th century  
11 European daily temperature and precipitation series, Int. J. Climatol., 23, 679-692, 2003.

12 Wild, M.: Global dimming and brightening: A review, J. Geophys. Res., 114, D00D16, 2009.

13 Wild, M.: Enlightening global dimming and brightening, Bull. Amer. Meteor. Soc., 93, 27–  
14 37, 2012.

15 Wild, M., Gilgen, H., Roesch, A., Ohmura, A., Long, C. N., Dutton, E. G., Forgan, B., Kallis,  
16 A., Russak, V., and Tsvetkov, A.: From dimming to brightening: Decadal changes in solar  
17 radiation at Earth’s surface, Science, 308, 847-850, 2005.

18 Wild, M., Trüssel, B., Ohmura, A., Long, C. N., Dutton, E. G., König-Langlo, G., and  
19 Tsvetkov, A.: Global dimming and brightening: An update beyond 2000, J. Geophys. Res.,  
20 114, D00D13, 2009.

21 WMO (World Meteorological Organization): Guide to meteorological instruments and  
22 methods of observation, 7th Edn. WMO Publication 8, Geneva, Switzerland, 2008.

23 WMO (World Meteorological Organization): WMO Scientific Assessment of Ozone  
24 Depletion: 2010, Global Ozone Research and Monitoring Project, Report No 52, World  
25 Meteorological Organization, Geneva, Switzerland, 2011.

26

27

28

29



1 **Tables**

2 Table 1: Characteristics of the AEMet stations used, and number of data used by different  
3 models and measurements to form the reconstructed UVER series. The total number of data  
4 and the year when the reconstructed series began are included.

Location	Latitude	Longitude	Altitude (m.s.l)	Model SW	Model F	Measured data	Total	First year
Ciudad Real	38°59'21''N	3°55'13''W	628	5717	9300	6	15023	1970
San Sebastián	43°18'23''N	2°02'28''W	251	7428	15029	9	22466	1950
A Coruña	43°21'57''N	8°25'17''W	58	9600	11388	2	20990	1951
Madrid	40°27'06''N	3°43'27''W	664	13208	9158	7	22373	1950
Cáceres	39°28'17''N	6°20'20''W	394	9517	1054	7	10578	1983
Murcia	38°00'07''N	1°10'15''W	61	10035	101	0	10136	1984
Tortosa	40°49'14''N	0°29'29''E	44	5081	12476	15	17572	1954
Valladolid	41°39'00''N	4°46'00''W	735	6813	7139	16	13968	1973
Villalba	41°48'50''N	4°55'48''W	840	3712	18180	0	21892	1951

5  
6  
7  
8  
9  
10  
11  
12  
13  
14  
15

1 Table 2: Statistical estimators calculated with N pairs of measured and reconstructed UVER  
 2 radiation for M-SW and M-F models and for different temporal resolutions. The hourly values  
 3 were obtained using data with SZA below 80°.

Resolution	Model	N	MBE (%)	RMSE (%)
Hourly	M-SW	220105	1.6	15.8
Daily	M-SW	21349	1.5	8.4
Daily	M-F	21349	5.1	24.7
Monthly	M-SW	845	1.8	5.2
Monthly	M-F	783	2.3	6.4
Annual	M-SW	38	0.3	2.9
Annual	M-F	35	-0.6	2.6

4  
 5  
 6  
 7  
 8  
 9  
 10  
 11  
 12  
 13  
 14  
 15  
 16  
 17  
 18  
 19

1 Table 3: Statistically significant UVER irradiation trends with a confidence of 99% (95%  
2 marked with an asterisk) and their 95% confidence interval, at different seasons and locations  
3 for the 1950-2011, 1950-1984, and 1985-2011 periods.  $TS_{O_3}$  and  $TS_{ac}$  are also included. N is  
4 the number of data used.

Location	Period	Season	N	TS ( $Jm^{-2}dc^{-1}$ )	TS (% $dc^{-1}$ )	$TS_{O_3}$ ( $Jm^{-2}dc^{-1}$ )	$TS_{ac}$ ( $Jm^{-2}dc^{-1}$ )	95CI ( $Jm^{-2}dc^{-1}$ )
Ciudad Real	1950-2011	Spring	41	78	2.59	64	14	(15:140)
Ciudad Real	1950-2011	Summer	41	90	1.88	46	44	(26:153)
Ciudad Real	1950-2011	Annual	41	49	1.86	30	19	(19:76)
Ciudad Real	1985-2011	Summer	27	207	4.31	61	146	(52:310)
Ciudad Real	1985-2011	Annual	27	71	2.67	28	43	(23:123)
San Sebastián	1950-2011	Spring	62	42	1.98	42	0	(9:75)
San Sebastián	1950-2011	Summer	61	59	1.81	59	0	(23:92)
San Sebastián*	1950-2011	Autumn	62	13	0.96	4	9	(-2:27)
San Sebastián	1950-2011	Annual	62	28	1.56	29	-1	(10:46)
San Sebastián*	1950-1984	Winter	35	-15	-2.97	2	-17	(-27:1)
San Sebastián	1950-1984	Spring	35	-109	-5.40	-33	-76	(-173:-31)
San Sebastián	1950-1984	Annual	35	-48	-2.76	-5	-43	(-79:-15)
San Sebastián*	1985-2011	Spring	27	100	4.46	64	36	(-1:202)
San Sebastián	1985-2011	Summer	27	164	4.85	88	76	(58:269)
San Sebastián*	1985-2011	Annual	27	68	3.68	45	23	(3:114)
A Coruña*	1950-2011	Spring	57	34	1.47	30	4	(1:71)
A Coruña	1950-2011	Summer	56	67	1.85	41	26	(27:111)
A Coruña	1950-2011	Annual	58	28	1.41	20	8	(11:42)
A Coruña*	1950-1984	Spring	30	-86	-3.93	-21	-65	(-164:9)
A Coruña*	1950-1984	Annual	31	-34	-1.82	-1	-33	(-76:5)
Madrid*	1950-2011	Summer	61	33	0.71	40	-7	(2:61)
Cáceres*	1950-2011	Spring	29	94	3.04	46	48	(11:206)
Cáceres	1950-2011	Summer	29	173	3.56	66	107	(56:275)
Cáceres	1950-2011	Annual	29	87	3.29	29	58	(41:125)
Cáceres	1985-2011	Summer	27	163	3.35	54	109	(23:295)
Cáceres	1985-2011	Annual	27	82	3.05	24	58	(32:120)
Murcia	1950-2011	Summer	28	138	3.04	2	136	(31:218)
Murcia*	1950-2011	Annual	28	44	1.71	-6	50	(-11:96)
Murcia	1985-2011	Summer	27	137	3.03	-6	143	(29:226)
Tortosa	1950-2011	Spring	48	48	1.78	51	-3	(10:79)
Tortosa	1950-2011	Summer	48	63	1.50	54	9	(29:99)
Tortosa	1950-2011	Annual	48	34	1.48	31	3	(15:54)
Tortosa	1985-2011	Summer	27	111	2.61	66	45	(23:205)
Valladolid	1950-2011	Winter	38	24	3.62	13	11	(5:45)
Valladolid	1950-2011	Spring	38	103	3.70	78	25	(43:174)
Valladolid	1950-2011	Summer	38	139	3.08	68	71	(53:193)
Valladolid	1950-2011	Annual	38	68	2.84	40	28	(36:97)
Valladolid*	1985-2011	Summer	27	137	2.98	65	72	(-11:280)
Valladolid*	1985-2011	Annual	27	56	2.28	30	26	(2:111)
Villalba	1950-2011	Winter	61	17	2.52	13	4	(6:29)
Villalba	1950-2011	Spring	61	47	1.70	47	0	(10:85)
Villalba	1950-2011	Summer	60	53	1.16	50	3	(19:84)
Villalba	1950-2011	Annual	61	30	1.25	30	0	(13:47)
Villalba*	1985-2011	Summer	27	130	2.79	63	67	(6:257)
Villalba*	1985-2011	Autumn	27	83	4.94	-1	84	(6:128)
Villalba*	1985-2011	Annual	27	63	2.54	31	32	(2:125)
Iberian Peninsula	1950-2011	Spring	62	33	1.19	38	-5	(4:62)
Iberian Peninsula	1950-2011	Summer	62	54	1.25	46	8	(26:78)
Iberian Peninsula	1950-2011	Annual	62	25	1.05	24	1	(12:38)
Iberian Peninsula	1985-2011	Summer	27	109	2.47	46	63	(24:206)

Location	Period	Season	N	TS ( $\text{Jm}^{-2}\text{dc}^{-1}$ )	TS ( $\%\text{dc}^{-1}$ )	TS <sub>o3</sub> ( $\text{Jm}^{-2}\text{dc}^{-1}$ )	TS <sub>ac</sub> ( $\text{Jm}^{-2}\text{dc}^{-1}$ )	95CI ( $\text{Jm}^{-2}\text{dc}^{-1}$ )
Iberian Peninsula*	1985-2011	Annual	27	50	2.09	19	31	(6:91)

- 1
- 2
- 3
- 4
- 5
- 6
- 7
- 8
- 9
- 10
- 11
- 12
- 13
- 14
- 15
- 16
- 17
- 18
- 19
- 20
- 21
- 22
- 23
- 24

1 Table 4: Statistically significant UVER irradiation trends considered as the median of 10,000  
2 trends (standard deviation in parenthesis), with a confidence of 99% (95% marked with an  
3 asterisk), and the P(p<0.05) and P(p<0.01) values at various locations and seasons for the  
4 1950-2011, 1950-1984, and 1985-2011 periods.

Location	Period	Season	TS (Jm <sup>-2</sup> dc <sup>-1</sup> )	TS (%dc <sup>-1</sup> )	P(p<0.05) (%)	P(p<0.01) (%)
Ciudad Real*	1950-2011	Spring	78 (5.9)	2.59 (0.19)	99.98	73.97
Ciudad Real*	1950-2011	Summer	88 (8.8)	1.84 (0.19)	99.99	91.96
Ciudad Real	1950-2011	Annual	48 (3.2)	1.81 (0.12)	100	99.98
Ciudad Real*	1985-2011	Summer	189 (17.9)	3.92 (0.37)	99.99	91.40
Ciudad Real*	1985-2011	Annual	73 (5.7)	2.75 (0.21)	100	98.52
San Sebastián*	1950-2011	Spring	41 (3.0)	1.95 (0.14)	99.98	57.53
San Sebastián	1950-2011	Summer	60 (4.5)	1.83 (0.14)	100	99.97
San Sebastián	1950-2011	Annual	28 (1.5)	1.54 (0.08)	100	100
San Sebastián*	1950-1984	Spring	-106 (9.2)	-5.24 (0.46)	100	99.01
San Sebastián*	1950-1984	Annual	-46 (4.4)	-2.63 (0.25)	100	95.18
San Sebastián	1985-2011	Summer	161 (12.7)	4.76 (0.38)	100	99.46
San Sebastián*	1985-2011	Annual	67 (4.4)	3.56 (0.24)	99.19	21.76
A Coruña	1950-2011	Summer	68 (4.3)	1.86 (0.12)	100	100
A Coruña	1950-2011	Annual	27 (1.4)	1.39 (0.07)	100	100
Cáceres*	1950-2011	Spring	95 (8.3)	3.06 (0.27)	100	30.58
Cáceres	1950-2011	Summer	177 (12.1)	3.65 (0.25)	100	99.96
Cáceres	1950-2011	Annual	88 (3.5)	3.28 (0.13)	100	100
Cáceres*	1985-2011	Summer	168 (14.0)	3.45 (0.29)	99.97	83.57
Cáceres	1985-2011	Annual	79 (4.4)	2.96 (0.16)	100	100
Murcia*	1950-2011	Summer	136 (10.2)	3.00 (0.23)	100	94.61
Murcia*	1985-2011	Summer	135 (10.9)	2.99 (0.24)	99.99	78.76
Tortosa*	1950-2011	Spring	46 (4.1)	1.72 (0.16)	99.51	51.72
Tortosa	1950-2011	Summer	65 (6.0)	1.56 (0.14)	100	99.91
Tortosa	1950-2011	Annual	34 (2.1)	1.48 (0.09)	100	100
Valladolid*	1950-2011	Winter	24 (2.2)	3.62 (0.34)	99.93	69.07
Valladolid	1950-2011	Spring	103 (7.2)	3.71 (0.26)	100	99.98
Valladolid	1950-2011	Summer	130 (10.3)	2.87 (0.23)	100	99.94
Valladolid	1950-2011	Annual	68 (3.2)	2.83 (0.13)	100	100
Villalba	1950-2011	Winter	17 (1.4)	2.57 (0.20)	100	99.78
Villalba*	1950-2011	Spring	47 (4.2)	1.68 (0.15)	99.80	62.46
Villalba*	1950-2011	Summer	55 (7.1)	1.20 (0.16)	99.79	91.98
Villalba	1950-2011	Annual	31 (2.3)	1.26 (0.10)	100	99.99
Iberian Peninsula*	1950-2011	Spring	33 (1.9)	1.22 (0.07)	100	41.45
Iberian Peninsula	1950-2011	Summer	54 (2.7)	1.25 (0.06)	100	100
Iberian Peninsula	1950-2011	Annual	25 (0.9)	1.05 (0.04)	100	100
Iberian Peninsula*	1985-2011	Summer	111 (6.1)	2.53 (0.14)	100	94.36
Iberian Peninsula*	1985-2011	Annual	50 (2.1)	2.06 (0.09)	100	36.93

5  
6  
7  
8  
9

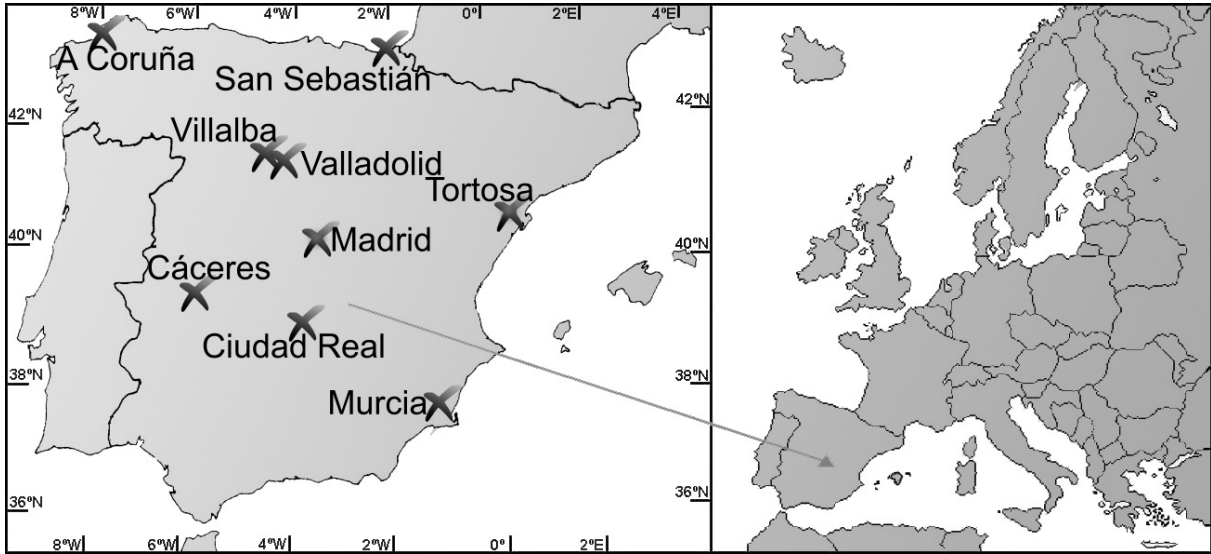
1 Table 5: Statistically significant UVER<sub>ob</sub> irradiation trends with a confidence of 99% (95%  
2 marked with an asterisk) and their 95% confidence interval, at different seasons and locations  
3 for the 1950-2011, 1950-1984, and 1985-2011 periods. N is the number of data used.

Location	Period	Season	N	TS (Jm <sup>-2</sup> dc <sup>-1</sup> )	TS (%dc <sup>-1</sup> )	95CI (Jm <sup>-2</sup> dc <sup>-1</sup> )
Ciudad Real*	1950-2011	Winter	41	5	3.18	(0:10)
Ciudad Real	1950-2011	Spring	41	57	7.28	(32:80)
Ciudad Real	1950-2011	Summer	41	119	6.42	(93:146)
Ciudad Real*	1950-2011	Autumn	41	14	2.42	(0:27)
Ciudad Real	1950-2011	Annual	41	49	5.78	(38:61)
Ciudad Real	1950-1984	Summer	14	141	8.35	(55:262)
Ciudad Real*	1985-2011	Spring	27	43	5.25	(-1:89)
Ciudad Real	1985-2011	Summer	27	107	5.55	(46:170)
Ciudad Real	1985-2011	Annual	27	41	4.64	(18:63)
San Sebastián	1950-2011	Spring	62	14	2.73	(1:25)
San Sebastián	1950-2011	Summer	61	26	2.64	(10:40)
San Sebastián	1950-2011	Annual	62	11	2.29	(5:18)
San Sebastián	1950-1984	Spring	35	-36	-7.57	(-56:-16)
San Sebastián	1950-1984	Annual	35	-16	-3.41	(-28:-5)
San Sebastián	1985-2011	Summer	27	69	6.54	(25:111)
San Sebastián	1985-2011	Annual	27	26	5.00	(7:43)
A Coruña*	1950-2011	Winter	59	2	1.44	(0:4)
A Coruña	1950-2011	Spring	57	15	2.62	(4:27)
A Coruña	1950-2011	Summer	56	36	3.24	(20:51)
A Coruña	1950-2011	Autumn	56	8	2.03	(3:12)
A Coruña	1950-2011	Annual	58	15	2.70	(9:19)
A Coruña	1950-1984	Spring	30	-26	-4.95	(-47:-6)
Madrid	1950-2011	Summer	61	40	2.35	(23:58)
Madrid	1950-2011	Annual	62	14	1.85	(7:21)
Cáceres	1950-2011	Spring	29	57	6.87	(8:92)
Cáceres	1950-2011	Summer	29	86	4.53	(36:144)
Cáceres	1950-2011	Annual	29	38	4.42	(16:56)
Cáceres*	1985-2011	Spring	27	40	4.78	(-8:81)
Cáceres	1985-2011	Summer	27	68	3.53	(18:140)
Cáceres	1985-2011	Annual	27	32	3.60	(11:50)
Murcia	1950-2011	Summer	28	127	6.63	(76:183)
Murcia	1950-2011	Annual	28	51	5.47	(29:70)
Murcia	1985-2011	Summer	27	122	6.30	(63:175)
Murcia	1985-2011	Annual	27	45	4.87	(25:64)
Tortosa	1950-2011	Spring	48	26	3.40	(12:41)
Tortosa	1950-2011	Summer	48	70	4.13	(57:91)
Tortosa	1950-2011	Autumn	48	12	2.09	(3:21)
Tortosa	1950-2011	Annual	48	29	3.59	(21:38)
Tortosa*	1950-1984	Summer	21	32	2.01	(-8:68)
Tortosa	1985-2011	Summer	27	91	5.05	(45:154)
Tortosa	1985-2011	Annual	27	38	4.56	(17:59)
Valladolid*	1950-2011	Winter	38	5	4.19	(0:9)
Valladolid	1950-2011	Spring	38	46	7.03	(24:70)
Valladolid	1950-2011	Summer	38	71	4.70	(41:102)
Valladolid*	1950-2011	Autumn	39	11	2.50	(-2:23)
Valladolid	1950-2011	Annual	38	34	4.98	(22:44)
Valladolid*	1950-1984	Autumn	12	50	11.28	(-14:132)
Valladolid*	1985-2011	Spring	27	38	5.48	(-1:81)
Valladolid*	1985-2011	Summer	27	48	3.07	(7:102)
Valladolid	1985-2011	Annual	27	26	3.62	(4:44)
Villalba	1950-2011	Winter	61	3	2.96	(1:6)
Villalba*	1950-2011	Spring	61	13	2.16	(1:27)

Location	Period	Season	N	TS ( $\text{Jm}^{-2}\text{dc}^{-1}$ )	TS ( $\%\text{dc}^{-1}$ )	95CI ( $\text{Jm}^{-2}\text{dc}^{-1}$ )
Villalba	1950-2011	Summer	60	27	1.87	(15:39)
Villalba	1950-2011	Annual	61	11	1.76	(5:17)
Villalba*	1950-1984	Spring	34	-29	-4.81	(-55:-2)
Villalba*	1985-2011	Annual	27	20	2.94	(0:42)
Iberian Peninsula*	1950-2011	Winter	62	2	1.50	(0:4)
Iberian Peninsula	1950-2011	Spring	62	14	2.02	(4:26)
Iberian Peninsula	1950-2011	Summer	62	37	2.35	(22:48)
Iberian Peninsula	1950-2011	Annual	62	15	2.02	(9:21)
Iberian Peninsula	1950-1984	Spring	35	-26	-4.25	(-50:-6)
Iberian Peninsula*	1950-1984	Annual	35	-10	-1.52	(-23:2)
Iberian Peninsula*	1985-2011	Spring	27	34	4.62	(-1:66)
Iberian Peninsula	1985-2011	Summer	27	59	3.63	(23:109)
Iberian Peninsula	1985-2011	Annual	27	28	3.75	(8:46)

1  
2  
3  
4  
5  
6  
7  
8  
9  
10  
11  
12  
13  
14  
15  
16  
17  
18  
19

1 **Figures**



2

3 Figure 1: Distribution of selected Spanish stations located in the Iberian Peninsula.

4

5

6

7

8

9

10

11

12

13

14

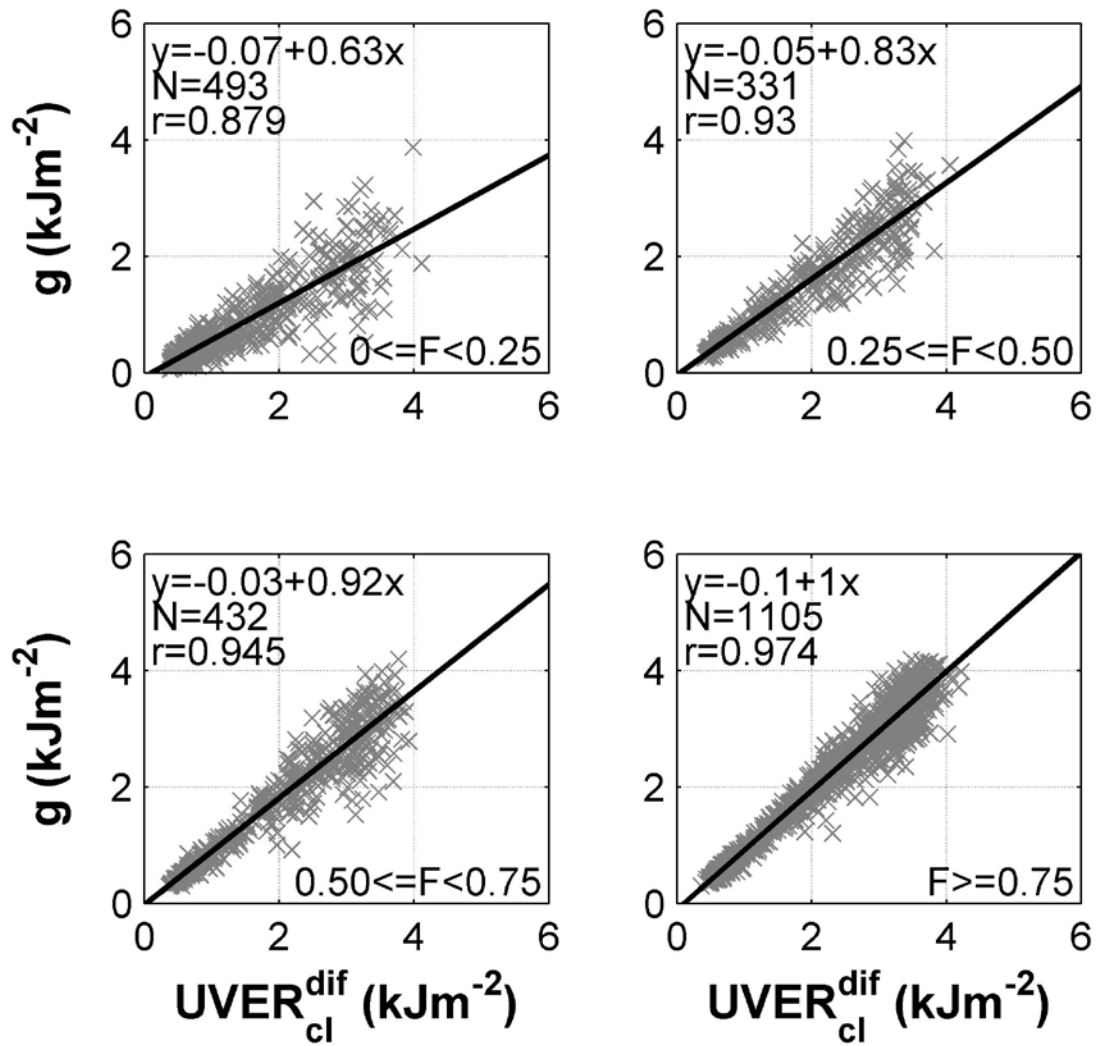
15

16

17

18





1

2 Figure 2: the  $g$  function against the simulated diffuse UVER under cloudless conditions for  
 3 four sunshine fraction (F) intervals. A linear fit calculated with the N data, and its equation  
 4 and correlation coefficient (r) are included in each panel.

5

6

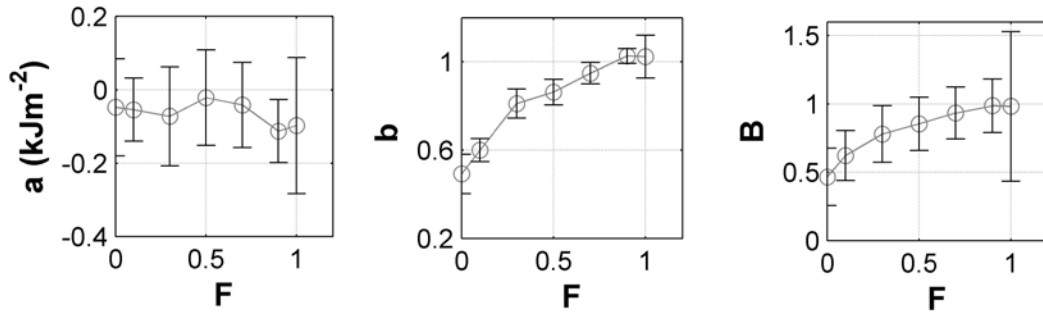
7

8

9

10

11



1

2 **Figure 3: Parameters  $a$  (left),  $b$  (middle), and  $B$  (right) calculated for different sunshine**  
 3 **fraction ( $F$ ) intervals. The error bar represents the combined uncertainty.**

4

5

6

7

8

9

10

11

12

13

14

15

16

17

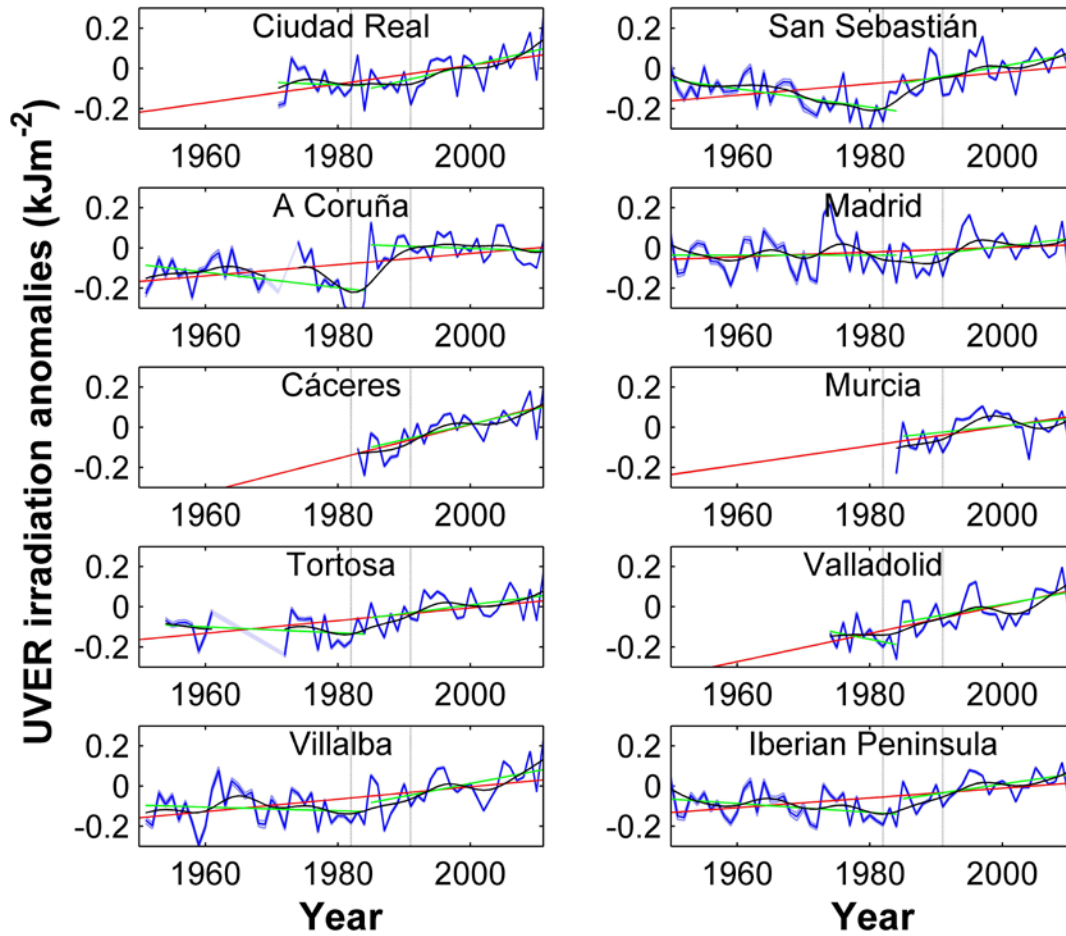
18

19

20

21

22



1

2 Figure 4: Evolution of the annual UVER irradiation anomalies and their uncertainties for ten  
 3 series. The red line corresponds to a linear fit between 1950 and 2011, and green lines to  
 4 linear fits in the 1950-1984 and 1985-2011 periods. The solid black line is a 21-year Gaussian  
 5 low-pass filter, and the years 1982 and 1991 are marked with a dashed black line.

6

7

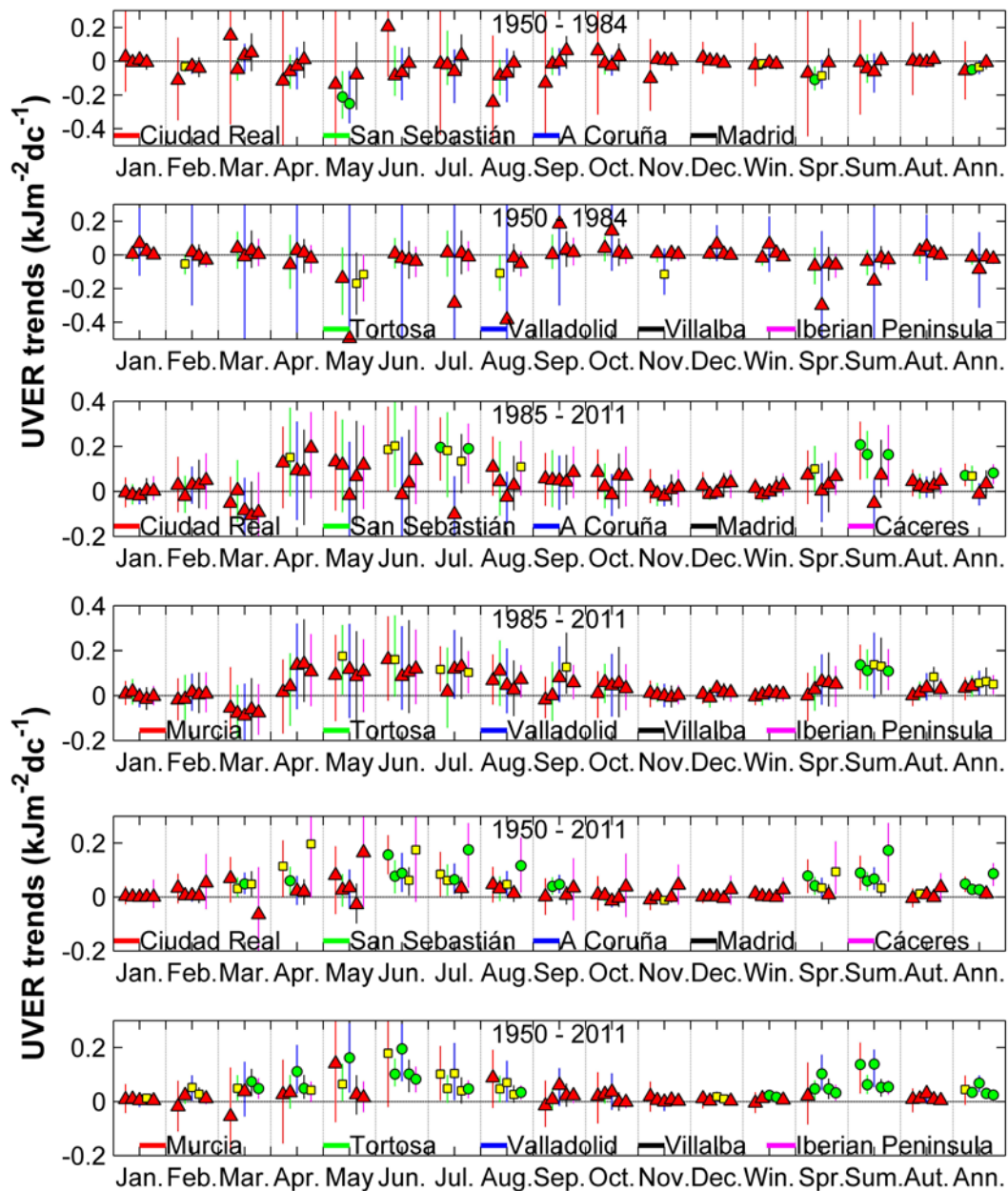
8

9

10

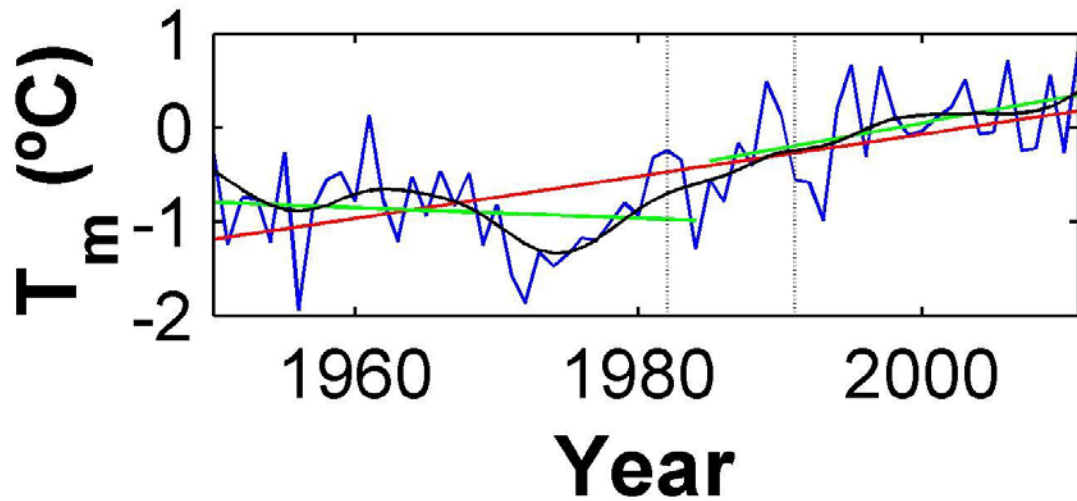
11

12



1  
 2 Figure 5: UVER trends for different months, seasons, and for annual and three periods. The  
 3 error bars are the 95% confidence interval and their colour represents the location of the  
 4 legend. The green circles represent statistically significant trends with 99% confidence  
 5 ( $p < 0.01$ ), yellow squares represent statistically significant trends with 95% confidence  
 6 ( $p < 0.05$ ), and red triangles represent non-statistically significant trends with at least 95%  
 7 confidence.

8



1

2 Figure 6: Evolution of the annual mean temperature anomalies and its uncertainties for the  
 3 Iberian Peninsula series. The red line corresponds to a linear fit between 1950 and 2011, and  
 4 green lines to linear fits in the 1950-1984 and 1985-2011 periods. The solid black line is a 21-  
 5 year Gaussian low-pass filter, and the years 1982 and 1991 are marked with a dashed black  
 6 line.

7

8

9

10

11

12

13

14

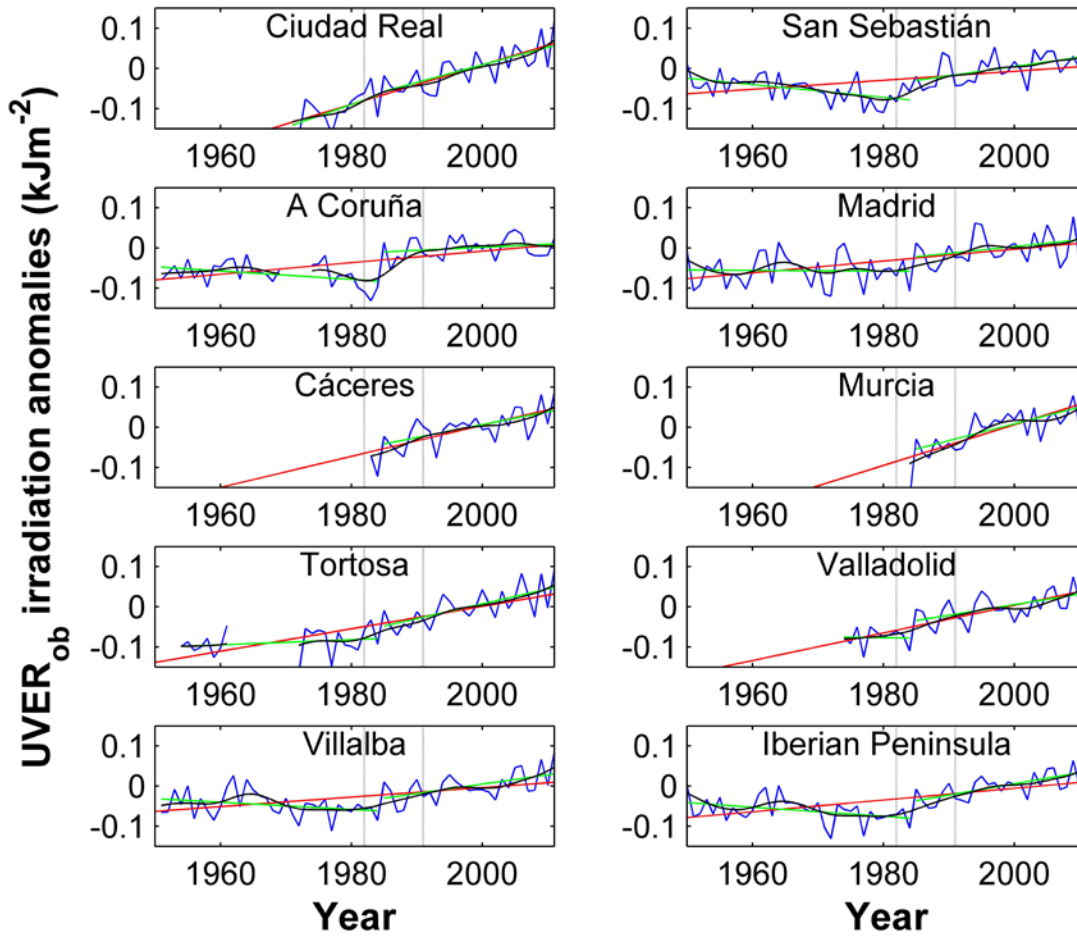
15

16

17

18

19



1

2 Figure 7: Evolution of the annual  $UVER_{ob}$  irradiation anomalies and their uncertainties for ten  
 3 series. The red line corresponds to a linear fit between 1950 and 2011, and green lines to  
 4 linear fits in the 1950-1984 and 1985-2011 periods. The solid black line is a 21-year Gaussian  
 5 low-pass filter, and the years 1982 and 1991 are marked with a dashed black line.

6

7

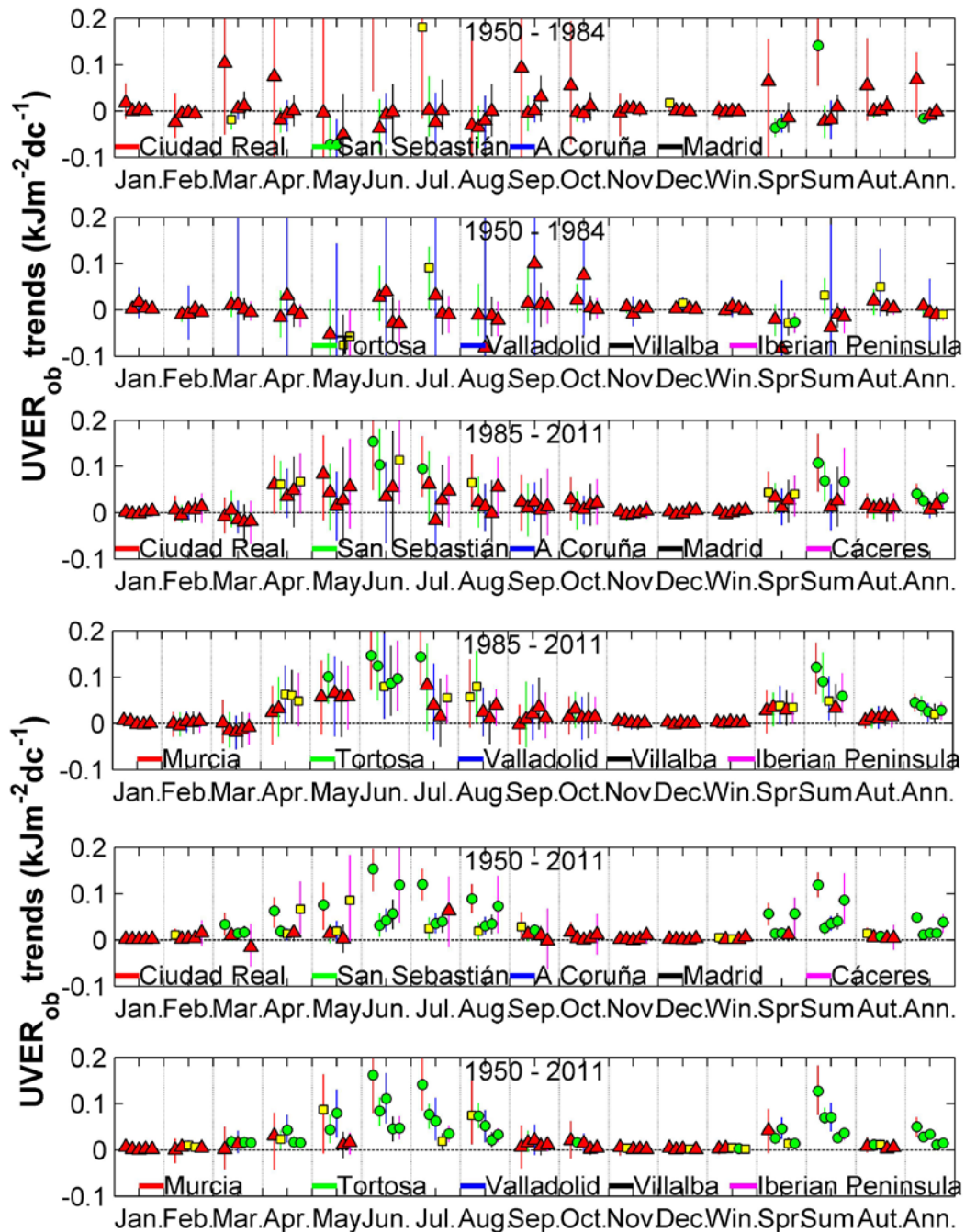
8

9

10

11

12



1  
2 Figure 8:  $UVER_{ob}$  trends for different months, seasons, and for annual and three periods. The  
3 error bars are the 95% confidence interval and their colour represents the location of the  
4 legend. The green circles represent statistically significant trends with 99% confidence  
5 ( $p < 0.01$ ), yellow squares represent statistically significant trends with 95% confidence  
6 ( $p < 0.05$ ), and red triangles represent non-statistically significant trends with at least 95%  
7 confidence.